Containment Air Cooler Heat Transfer During Loss of Coolant Accident With Loss of Offsite Power

November 1996

Prepared by
NUMERICAL APPLICATIONS, INC.
825 Goethals Drive, Suite A
Richland, Washington 99352

Principal Investigator
Thomas L. George

Prepared for
Electric Power Research Institute
3412 Hillview Avenue
Palo Alto, California 94303

EPRI Project Manager
Avtar Singh

Safety and Reliability Assessment Target
Nuclear Power Group

DISCLAIMER OF WARRANTIES AND LIMITATION OF LIABILITIES

ORGANIZATION(S) THAT PREPARED THIS REPORT

Numerical Applications, Inc.

For further information on licensing terms and conditions for this report, contact the EPRI project manager, Avtar Singh, at (415) 855-2384.

REPORT SUMMARY

Containment Air Cooler Heat Transfer During a Loss of Coolant Accident with Loss of Offsite Power

In this interim report, a selection of heat and mass transfer correlations from the reference literature is presented for predicting the thermal performance of finned horizontal tube bundles in cross flow of air steam mixtures in containment air coolers(CAC). For the tube exterior, considered heat transfer modes include laminar and turbulent convection and condensation. Heat transfer on the tube interior includes free and forced convection, subcooled and saturated pool boiling and subcooled and saturated boiling with forced convection. The correlation set is compared with the models existing in GOTHIC 5.0e. Methodologies are recommended for using GOTHIC to calculate the time to boiling in the tubes and the growth of the steam region in and around the CAC tubes.

BACKGROUND The Nuclear Regulatory Commission has issued a Generic Letter (GL 96-06) regarding the operation of containment air coolers (CAC) under certain conditions that may result in boiling of the water on the secondary side of the cooler. One particular identified condition is the operation of the CAC during LOCA with a concurrent Loss of Offsite Power (LOOP).Under this scenario, the fan on the primary side and the pump on the secondary side loose power during the LOCA. The water flow on the secondary side stops almost immediately but the fan coasts down slowly and continues to drive hot air and steam through the cooler. Depending on the configuration of the CAC system, this can cause boiling in the CAC tubes. If a significant steam region develops in the CAC secondary system, the potential for damaging condensation induced or column rejoining waterhammer needs to be considered.

OBJECTIVES 1. To provide plant safety engineers with correlations and methodology that can be used to predict whether or not boiling will occur in a particular CAC configuration. 2. To provide a methodology for estimating the size of the steam region when boiling does occur. 3. To support utility submittals to the NRC in response to GL 96-06.

APPROACH Based on a review of the literature for interior and exterior heat and mass transfer in finned horizontal tube bundles in cross flow, a set of correlations is presented that can be used to calculate the heat up of the water in the tubes and the subsequent boiling rate. The correlations and the related methodology can be used to calculate the time to boil and the growth of the steam region. For some plants it is sufficient to demonstrate that the boiling point is not reached before flow is restored to the secondary side. The time to boil methodology can also be used to determine the amount of pressurization required in the secondary system to prevent boiling

while the secondary side pumps are idle. For other plants, where boiling cannot be precluded, the methodology can be used to estimate the maximum size of the steam region that develops before and during the to the pump restart. This information is needed to estimate pressure spike that can occur when the steam region collapses due to rapid condensation. The magnitude of the pressure spike is needed to calculate the water hammer loads on the piping system.

RESULTS A recommended set of correlations and methodology is presented. The recommended approach is compared with the models used in the GOTHIC code for CAC analysis. The GOTHIC modeling approach takes advantage of the benchmarked CAC heat and mass transfer models and the full range of single phase and boiling heat transfer models for the secondary side. Using the described methodology, graphical results are presented for the time to boil versus the operating tube pressure for a typical CAC configuration. The simple model can be quickly constructed and may satisfy the need for some plants to resolve GL 96-06 issues. Noding studies were performed for a simplified complete secondary system to determine the number and location of computational cells needed to adequately model the development of the steam region. From this study it was determined that the processes was best represented with multidimensional noding in the manifolds and piping close to the CAC unit. Although the correlation set and methodology are based on accepted and experimentally verified components, there has not been any experimental validation of the models and methods as a whole. Experimental data that capture the essential features of the heat up and boiling process are needed to validate the recommended methodology. Such experiments are planned to be conducted as part of a proposed supplementary funded EPRI/industry collaborative project.

ACKNOWLEDGMENTS Funding for this study was provided by the EPRI supplementary funded Project for GOTHIC Development and Enhancements under the direction of the GOTHIC Advisory Group.

For availability information about this report, please contact EPRI project manager:

Avtar Singh
Electric Power Research Institute
3412 Hillview Avenue
Palo Alto, California 94304

Telephone: (415)-855-2384
Fax: (415)-855-1026
e-mail: AVSINGH@eprinet.epri.com

TABLE OF CONTENTS

LIST OF TABLES

LIST OF FIGURES

1. INTRODUCTION

This technical note describes heat transfer methodology to calculate the thermal response of a containment air cooler (CAC) during LOCA conditions with concurrent loss of offsite power (LOOP).

With a loss of offsite power, both the water pump on the secondary side and the fan on the air side of the CAC loose power and coast down. The pump has little inertia and coasts down within a couple of seconds. However, the CAC fan coasts down over a period of about 30 seconds. During this coast down period, and before diesel generator power is restored to the pump, there is potential for boiling the water in the CAC tubes by the high temperature air/steam mixture entering the CAC. The resulting steam region may result in damaging water hammer if it collapses rapidly after the pump is restarted.

The correlations and methodology described in this note will be useful for predicting whether or not the water in the tubes will start to boil before the circulation pumps are restarted and, if boiling does occur, the extent and location of the resulting steam region.

The CAC systems vary considerably from plant to plant and even from train to train within one plant. The absolute pressure in the tubes during LOCA with LOOP conditions is, of course, the major determining factor for boiling. If the system is, or can be, pressurized to a pressure above the saturation pressure at the peak containment temperatures during postulated LOCA's and MSLB's then there is no possibility of boiling. In all other cases some analysis must be done to estimate the time to boil and, if necessary, the size of the steam filled region at the time of pump restart.

The analysis starts with the water/tube/air/steam system

shown in the diagram below.

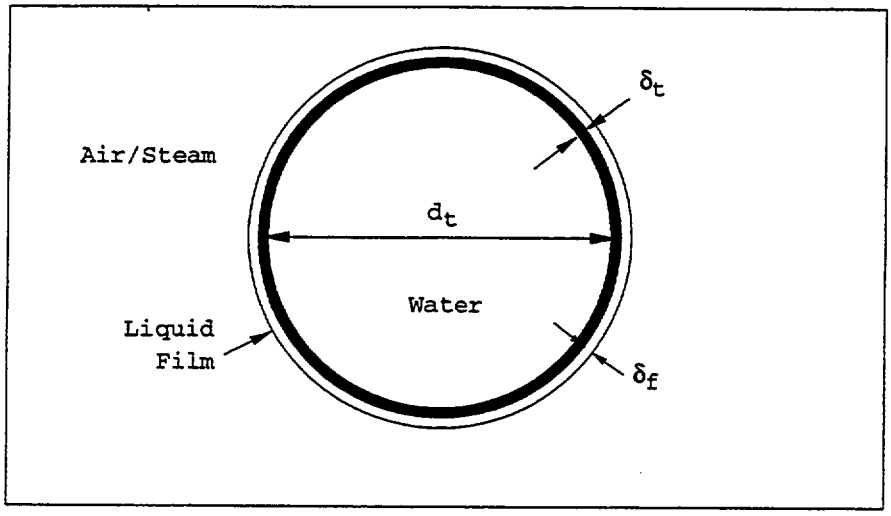

Figure 1.1 Tube Geometry

On the outside surface of the tube there will be condensation of the steam and convective heat transfer from the air/steam mixture (referred to here as vapor) driven by the coasting fan. A liquid film will develop on the heat transfer surfaces. On the inside, the water quickly becomes stagnant and will initially be heated either by conduction or by natural convection. If the temperature of the inner surface of the tube rises above the saturation temperature of the water in the tube, the heat transfer at the inner surface of the tube will be augmented by nucleate boiling. Further heating of the water will raise the water temperature to the saturation temperature and bulk boiling will occur.

Once boiling begins, the pressure in the tubes will rise as the steam bubbles expand and force water out of the CAC. This rise in pressure will retard the boiling to some extent. Some of the steam forced out of the CAC tubes will condense in the inlet and outlet headers and manifolds. The amount of condensation that will occur before a stable hot water interface is formed depends on the geometry of the inlet and outlet piping. The ultimate size of the

steam region is therefore dependent on the dynamics of the entire secondary system, the piping configuration near the CAC and the heat transfer in the CAC.

2. ASSUMPTIONS

Major assumption in this modeling approach are listed below.

1. The heat transfer from the air/steam mixture can be calculated using correlations for averaged heat transfer around the circumference of the tube and averaged for the tube bank. For typical tube sizes, the thermal time constant for circumferencial heat conduction in the tube wall is on the order of 1 second. This is short relative to the time span of interest (20-30 seconds) and will tend to keep conditions uniform around the tube circumference.

2. Steady state heat transfer correlations will be used. The length scale for the tube heat transfer is small and the response time to changes in bulk and surface conditions is short relative to the time span of interest.

3. The water in the tubes is initially stagnant. This is not a necessary assumption but pump coast times are usually not available and are known to be short. This assumption results in a conservative time to boil estimate.

3. OUTSIDE TUBE HEAT TRANSFER

The tube geometry for a CAC typically is an array of parallel tubes with thin sheet fins perpendicular to the tube axes. The tubes are usually staggered as shown in Figure 3.1a, but may be in-line as in 3.1b. The air/steam mixture flows across the tube array between the plate fins. The flow rate of the air/steam mixture is controlled by the CAC fan.

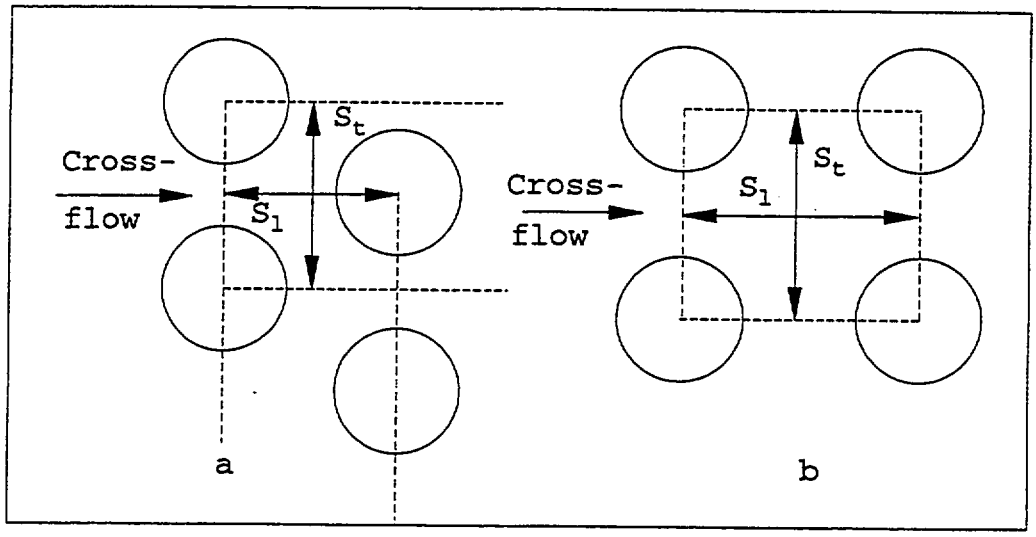

Figure 3.1 Tube Bundle Geometries

As the steam concentration increases in the containment, the heat transfer rate on the air side of the CAC is quickly dominated by the condensation on the tube and fin surfaces. The condensation rate is generally limited by the diffusion through the air boundary layer that builds up on the condensing surfaces.

For condensation heat transfer, the total heat rate to the condensing surface is the sensible heat transfer due to convection plus the heat of vaporization given up by the condensing steam, i.e., (see, e.g., [Collier, 1981])

$$Q'' = Q''_{conv} + Q''_{cond} \qquad (3.1)$$

Each of these components is considered separately below.

3.1. Convection Heat Transfer

For turbulent convective heat transfer to tube bundles in crossflow, the convective heat transfer coefficients recommended in [Hdbk of Conv HT,1987] for inline tube bundles are

$$Nu_h = 0.9\ Re^{0.4}\ Pr^{0.36}\left(\frac{Pr}{Pr_s}\right)^{0.25} \qquad 0<Re<241 \qquad (3.2)$$

$$Nu_h = 0.52\ Re^{0.5}\ Pr^{0.36}\left(\frac{Pr}{Pr_s}\right)^{0.25} \qquad 241<Re<900 \qquad (3.3)$$

$$Nu_h = 0.27\ Re^{0.63}\ Pr^{0.36}\left(\frac{Pr}{Pr_s}\right)^{0.25} \qquad 1000<Re<200,000 \qquad (3.4)$$

and for staggered tube bundles are

$$Nu_h = 1.04\ Re^{0.4}\ Pr^{0.36}\left(\frac{Pr}{Pr_s}\right)^{0.25} \qquad 0<Re<46 \qquad (3.5)$$

$$Nu_h = 0.71\ Re^{0.5}\ Pr^{0.36}\left(\frac{Pr}{Pr_s}\right)^{0.25} \qquad 46<Re<900 \qquad (3.6)$$

$$Nu_h = 0.35\left(\frac{S_t}{S_l}\right)^{0.2} Re^{0.6}\ Pr^{0.36}\left(\frac{Pr}{Pr_s}\right)^{0.25} \qquad 1000<Re<200,000 \qquad (3.7)$$

These correlations require that the hydraulic diameter be set to the tube OD. The velocity in the Reynolds number is the velocity at the minimum flow area between tubes. For gas mixtures the bulk-to-wall Prandtl Number ratio can be approximated by [Churchill, 1955]

$$\left(\frac{Pr}{Pr_s}\right)^{.25} = \left(\frac{T_v}{T_i}\right)^{.12} \qquad (3.8)$$

where T_v is the bulk vapor temperature and T_i is the liquid/vapor interface temperature.

For Reynolds numbers between 900 and 1000, linear interpolation is used to calculate the Nusselt number. The

accuracy of these correlations is estimated at ±15%.

These heat transfer correlations are for tube banks with ten or more rows in the direction of the flow. If there are fewer rows, the average heat transfer coefficient should be reduced by the factors in the table below
[Kays and Lo, 1952]

Table 3.1 Reduction Factors for Shallow Tube Banks

Number of Rows	Staggered Tubes	In-line Tubes
1	0.6800	0.6400
2	0.7500	0.8000
3	0.8300	0.8700
4	0.8900	0.9000
5	0.9200	0.9200
6	0.9500	0.9400
7	0.9700	0.9600
8	0.9800	0.9800
9	0.9900	0.9900
10	1.0000	1.0000

Using the correlations for the Nusselt number, the convective heat transfer coefficient between the air/steam mixture and the liquid/vapor interface is calculated as

$$H_{vi} = Nu_h \frac{k_v}{D} \tag{3.9}$$

and the convective heat transfer is

$$Q'' = H_{vi} \left(T_v - T_i \right) \tag{3.10}$$

The interface temperature is unknown and must be calculated by balancing the heat to and from the interface using the additional relationship given below.

3.2. Condensation

Using an analogy between heat and mass transfer, the condensation rate can be calculated from [Bird,1960]

$$\Gamma'' = \frac{H_m M_s}{1 - \phi_i}\left(\phi_i - \phi_v\right) \tag{3.11}$$

where H_m is the mass transfer coefficient, M_s is the steam molecular weight and ϕ_i and ϕ_v are the steam mole fractions at the liquid/vapor interface and the bulk vapor, respectively. Written in this form, $\Gamma''>0$ implies vaporization.

The heat/mass transfer analogy provides a method of calculating a mass transfer coefficient from a correlation for heat transfer. For forced convection the heat transfer coefficient is typically correlated as

$$Nu_h = f(Re, Pr) \tag{3.12}$$

Assuming that the mass transport process through the boundary layer is similar to the heat transport process, the same functional form may be used to calculate a mass transport coefficient if the Prandtl number is replaced by the Schmidt number, i.e.,

$$Nu_m = f(Re, Sc) \tag{3.13}$$

where

$$Nu_m = \frac{H_m D}{\chi \lambda} \tag{3.14}$$

In this mass transfer Nusselt number, λ is the binary gas diffusion coefficient and χ is the molar concentration of the bulk air/steam mixture.

For air/steam mixtures, the binary diffusion coefficient can be approximated using [Holman,1963]

$$\lambda = 0.0069\ T_v^{\frac{3}{2}}\ \frac{\sqrt{\frac{1}{M_s}+\frac{1}{M_a}}}{P\left(V_s^{\frac{1}{3}}+V_a^{\frac{1}{3}}\right)^2}\quad ft^2/hr \tag{3.15}$$

where T is in degrees R, the total pressure P is in atmospheres, and V_s=18.8 and V_a=29.9 are the molecular volumes for steam and air.

Using the functional form of Equations 3.2-3.7, with the Prandtl number replaced by the Schmidt number, the mass transfer coefficient can be calculated from Equation 3.14 and the rate of condensation calculated from Equation 3.11. The heat delivered to the condensing surface is

$$Q''_{cond} = -\Gamma''\ h_{lv} \tag{3.16}$$

where h_{lv} is the effective heat of vaporization.

The condensation rate depends on the steam mole fraction at the interface. It is usually assumed that the steam pressure at the interface is the saturation pressure at the interface temperature so that

$$\phi_i = \frac{P_{sat}\left(T_i\right)}{P} \tag{3.17}$$

To be able to model the full range of vapor and film conditions, including superheating and subcooling, it is assumed that

$$h_{lv} = h_{vs} - h_l \tag{3.18}$$

where h_{vs} is the bulk steam enthalpy and h_l is the liquid enthalpy at the liquid film temperature, T_f. This assumption implies that the heat delivered to the interface due to condensation is the heat released by bringing the steam from its current state (superheated or saturated) down to the film temperature which may be subcooled. It is further assumed that the film temperature is

$$T_f = \frac{T_i + T_{wo}}{2} \tag{3.19}$$

where T_{wo} is the temperature of the outer surface of the tube.

4. TUBE AND FILM HEAT TRANSFER

For thin films the heat transfer through the film can be calculated from

$$Q'' = \frac{k_l}{\delta_f}\left(T_i - T_{wo}\right) \tag{4.1}$$

where k_l is the liquid conductivity and δ_f is the film thickness. For condensation on a vertical flat plate, such as the fins in a CAC, the condensate film thickens from the top to the bottom of the plate as more condensate is added to the film flow. Neglecting the effects of drag on the film surface by the air/steam flow and assuming a constant condensation rate over the plate, the approach used by Nusselt [Kreith,1965] gives

$$\delta_f = \frac{3}{4}\left(\frac{3\,\mu\,\Gamma''\,L}{\rho_l^{\,2}\,g}\right)^{\frac{1}{3}} \tag{4.2}$$

for the average film thickness over a plate of height L.

In comparing the model described in this note as programmed in GOTHIC with experimental data for finned tube bundles, the above equation was found to predict films that were too thin and therefore resulted in over prediction of the heat transfer rate. Better agreement with the data was obtained using

$$\delta_f = 0.075\ Re^{-.6} \quad ft \tag{4.3}$$

For the CAC experiments analyzed (see Section 7.1), this expression gives average film thicknesses that are 1.5 to

4 times thicker than those given by Equation 4.2. It is postulated that the condensate tends to collect between the closely spaced fins at the tube surface and the vapor drag on the film surface is dominant in determining the thickness of this film on the tubes.

Conduction through the thin walled tube can be calculated from

$$Q'' = \frac{1}{F_i + \frac{\delta_t}{k_t} + F_o} \left(T_{wo} - T_{wi} \right) \tag{4.4}$$

where T_{wi} is the inside tube surface temperature and F_i and F_o are the inside and outside fouling factors.

4.1. Fins

Most CACs use finned bundles. The approach used to account for fins in heat exchangers can be extended to the case where there is condensation on the fin and tube surfaces. For a heat exchanger without phase change, the effect of fins can be accounted for in terms of a fin effectiveness coefficient defined as the ratio of the actual heat transfer from the fins to the heat transfer from the fins when the entire fin surface is at the tube temperature. The multiplier on the total heat transfer area (fins plus tubes) is given by

$$\eta_0 = 1 - \frac{A_{fin}}{A_{tot}} (1 - \eta) \tag{4.5}$$

where for plate fins

$$\eta = \frac{\tanh (m\, l)}{m\, l} \tag{4.6}$$

and

$$m = \sqrt{\frac{2\,H_{eff}}{k_{fin}\,\delta_{fin}}} \tag{4.7}$$

For plate fins prependicular to tube arrays, the fin length, 1, should be 1/2 the distance between adjacent tube walls ($.5*(S_l-d_t)$ for in-line tube bundles).

For heat exchangers without phase change, H_{eff} is the bundle average convection coefficient. In the case where there is condensation and a liquid film on the fin surface, the total heat to the fin is

$$Q'' = H_{eff}\left(T_v - T_{fin}\right) = H_{vi}\left(T_v - T_i\right) - \Gamma''\,h_{vl} \tag{4.8}$$

From Equation 3.11 and the assumption that the bulk air/steam mixture is saturated, the condensation rate can be estimated from

$$\Gamma'' = \frac{-H_m\,M_s}{\left(1. - \phi_i\right)P}\left(P_{sat}\left(T_v\right) - P_{sat}\left(T_i\right)\right) = \frac{-H_m\,M_s}{\left(1 - \phi_i\right)P}\frac{dP_{sat}}{dT}\left(T_v - T_i\right) \tag{4.9}$$

The heat flux to the fin surface is the same as the conduction through the film giving

$$Q'' = \frac{k_l}{\delta_f}\left(T_i - T_{fin}\right) \tag{4.10}$$

Combining the above gives

$$\frac{1}{H_{eff}} = \frac{1}{H_{vi}} + \frac{\left(1 - \phi_i\right)P}{H_m\,M_s\,\dfrac{dP_{sat}}{dT}} + \frac{\delta_f}{k_l} \tag{4.11}$$

for use in Equation 4.7.

5. INSIDE TUBE HEAT TRANSFER

Possible heat transfer modes inside the tube range from

developing free convection from stagnant water, forced laminar or turbulent convection as the water begins to move, subcooled or saturated nucleate boiling when the wall temperature reaches the saturation temperature, forced convection saturated boiling and free and forced convection to vapor. Correlations are presented below to address these heat transfer modes.

5.1. Free Convection to Liquid

Correlations for free convection inside a horizontal cylinder with uniform heating or surface temperature are difficult to obtain because the process is inherently unsteady. The correlation by [Hong, 1974] for water in tubes with finite peripheral conduction is accurate within ±10% over Grashof numbers ranging from 200 to 600000. The correlation is

$$Nu_N = 0.378\ Ra^{0.28}\ Pr^{0.05}\ f^{-0.12} \tag{5.1}$$

where Ra is Rayleigh Number

$$Ra = \frac{g\,\rho^2\,c_p\,\beta\left(T_w - T_l\right)D_h^{\,3}}{\mu\,k} \tag{5.2}$$

and

$$f = \frac{H\,D_h^{\,2}}{\delta_t\,k_t} \tag{5.3}$$

The Nusselt correlation can be more conveniently written as

$$Nu_N = 0.420\ Ra^{0.25}\ Pr^{0.045}\left(\frac{\delta_t\,k_t}{D_h\,k_l}\right)^{0.11} \tag{5.4}$$

The correlation was tested against data for water in metal and glass tubes. It is not known if the correlation is still valid for copper tubing since it has a very high conductivity. An alternative correlation by Evans and

Stefany [Hdbk of HT Fund, 1985] is

$$Nu_N = 0.55\ Ra^{0.25} \tag{5.5}$$

This correlation was tested against data for short horizontal cylinders for $7<Pr<700$ and $6x10^5<Ra<6x10^9$ with an accuracy of ±10%.

5.2. Forced Convection

Assuming constant wall temperature along the length of the tube, the laminar convection coefficient can be obtained from [Kays, 1967]

$$Nu_{LF} = 3.658 \tag{5.6}$$

For heating in turbulent flow in smooth tubes the Dittus-Boelter correlation is recommended [Hdbk of Heat Trans, 1973]

$$Nu_{TF} = 0.023\ Re^{0.8}\ Pr^{0.4} \tag{5.7}$$

and the general forced convection heat transfer coefficient is

$$Nu_F = Max\left(Nu_{LF}, Nu_{TF}\right) \tag{5.8}$$

5.2.1. Mixed Convection

In the mixed convection regime, the heat transfer coefficient is commonly obtained from [HEDH, 1989]

$$Nu^3 = Nu_N^{\ 3} + Nu_F^{\ 3} \tag{5.9}$$

5.3. Boiling Heat Transfer

For nucleate pool boiling in water [Collier, 1989] recommends a correlation based on the work of [Borishanski, 1969]

$$Q''_{NPB} = H_{NPB}\left(T_{wi} - T_{sat}\right) \tag{5.10}$$

with

$$H_{NPB} = 4.21\ Q''_{NPB}{}^{0.7} \left(1.8\ P_r{}^{0.17} + 4\ P_r{}^{1.2} + 10\ P_r{}^{10}\right) \qquad (5.11)$$

where

$$P_r = \frac{P}{P_c} \qquad (5.12)$$

In the above expressions, P is the water pressure, P_c is the critical pressure, Q" is in W/m^2, and H is in W/m^2-K. The influence of subcooling in the liquid is minor and the above expression can be used for saturated and subcooled nucleate boiling.

Once the water becomes saturated, the heat transfer mode will quickly enter a forced convection boiling regime as the generated vapor accelerates the two phase mixture out of the tubes. As long as the fluid does not enter a stratified flow regime, the Chen [Chen, 1966] correlation, developed for vertical flow should work well. In Chen's approach, the total heat transfer coefficient is the sum of a convective portion and a nucleate boiling component. The convective component is the Dittus-Boelter equation with a multiplier to account for two-phase effects.

$$H_{FC} = \frac{k_l}{D}\ 0.023\ Re_{tp}{}^{0.8}\ Pr^{0.4}\ Max\left(1.0, 2.35\left(\frac{1}{X_{tt}} + 0.213\right)^{0.736}\right) \qquad (5.13)$$

where X_{tt} is the Martinelli parameter

$$X_{tt} = \left(\frac{1-x}{x}\right)^{0.9} \left(\frac{\rho_v}{\rho_l}\right)^{0.5} \left(\frac{\mu_l}{\mu_v}\right)^{0.1} \qquad (5.14)$$

The nucleate boiling component is

$$H_{NB} = 0.00122\ S \frac{k_l{}^{0.79}\ c_p{}^{0.45}\ \rho_l{}^{0.49}}{\sigma^{0.5}\ \mu^{0.29}\ h_{fg}{}^{0.24}\ \rho_g{}^{0.24}} \Delta T_s{}^{0.24}\ \Delta P_s{}^{0.75} \qquad (5.15)$$

where

$$\Delta T_s = T_{wi} - T_l \tag{5.16}$$

and

$$\Delta P_s = P_{sat}\left(T_{wi}\right) - P_{sat}\left(T_l\right) \tag{5.17}$$

The boiling supression factor given by

$$S = \frac{1}{1 + 2.53 \times 10^{-6} \, Re_{tp}^{1.17}} \tag{5.18}$$

where the two phase Reynolds number is calculated as

$$Re_{tp} = \frac{G\,(1 - x)\,D}{\mu} \tag{5.19}$$

where G is the two phase mixture mass flux and x is the quality.

5.4. Single Phase Vapor

Once all of the water in the tube is expelled or boiled away, the remaining steam can still be heated to the containment temperature. The same correlations as used for the single phase liquid Nusselt number can be used to calculate the heat transfer coefficient for the vapor phase.

6. SOLUTION PROCEDURE

The above equations must be solved simultaneously to calculate the heat rate to the water. Unfortunately, the unknown tube surface temperatures and the liquid/vapor interface temperature cannot be eliminated by direct algebraic manipulations without making simplifying

assumptions that may compromise the solution. Typically, a multilevel iterative approach is needed to solve for the heat exchanger performance. Refer to the GOTHIC Technical Manual for one possible solution approach.

7. GOTHIC HEAT TRANSFER MODELS FOR CAC ANALYSIS

The CAC model in GOTHIC 5.0e is similar to that described above but there are some differences. For the outside tube heat transfer, the correlations are the same as presented above. For inside the tube heat transfer, the model is not as complete as that described above. The built in correlations for the secondary side assume forced turbulent convection only and no boiling. This would seem to indicate that the GOTHIC CAC model is not useful for the boiling problem. However, GOTHIC does include models for natural and forced convection and boiling in tubes that are not part of the CAC model. In this section, experimental verification is presented for the CAC model in steady state conditions and the GOTHIC correlations for heat transfer inside the tube are compared with the correlations listed in the preceding sections. In the next section a description is provided as to how the CAC model and the tube boiling models can be coupled together to solve the CAC boiling problem.

7.1. Condensation Heat Transfer in Finned Tube Bundles

The coupled modeling approach relies on the CAC model to predict the heat transfer on the outside of the tubes. To show the expected accuracy of this model, results are presented in this section for GOTHIC versus experimental data on heat transfer performance for CAC coils. The GOTHIC code was used to compare against experimental results obtained by American Air Filter [Rivers, 1972] for four different cooler coils. The tests covered expected conditions during LOCA without LOOP.

The four coil arrangements (Table 7.1) were typical of fan

cooler coils at the Palisades (PAL), Ft. Calhoun (FTC), Three Mile Island (TMI) and Oconee (OCO) plants.

Table 7.1 Coil Geometry.

M*

Parameter	PAL	FTC	TMI	OCO
Coil Depth (in)	18.5	18	12	12
Number of Rows	12	12	8	8
Fin Material	copper	aluminum	copper	aluminum
Fin Thickness (in)	0.007	0.0085	0.007	0.0085
Tube Wall Thickness (in)	0.049	0.022	0.049	0.049
Coolant Traverses	4	6	8	4

Tests were run for each coil at the conditions shown in Tables 7.2 and 7.3. The incoming air steam mixture was saturated at the specified temperature. Test measurements included the condensation rate, the primary and secondary side inlet and outlet temperatures and the primary and secondary side flow rates.

Table 7.2 AAF Test Vapor Inlet Conditions.

Plant	Run	Pres	Vapor Inlet	Sat Pres	Steam Frac
		psia	F	psia	
PAL	1	24.7	184.0	8.203	0.3321
	2	44.7	244.0	26.826	0.6001
	3	70.0	283.0	51.600	0.7371
FTC	4	24.7	185.0	8.384	0.3394
	5	44.7	244.0	26.826	0.6001
	6	74.7	288.0	55.795	0.7469
TMI	7	24.7	187.0	8.756	0.3545
	8	44.7	245.0	27.403	0.6130
	9	73.7	281.0	49.993	0.6783
OCO	10	24.7	184.0	8.203	0.3321
	11	44.7	244.0	26.826	0.6001
	12	73.7	286.0	54.083	0.7338

Array: aaf

Table 7.3 AAF Test Coolant Inlet Conditions.

M*

Plant	Run	Coolant Flow	Coolant Inlet	Vapor Flow
		$\frac{lbm}{min}$	F	$\frac{ft^3}{min}$
PAL	1	1652	99.5	1500.0
	2	1652	99.0	
	3	1672	100.0	
FTC	4	1200	120.0	2272.0
	5	1190	120.0	
	6	1152	120.0	
TMI	7	490	85.0	960.0
	8	482	85.0	
	9	476	85.5	
OCO	10	968	75.0	1800.0
	11	960	75.0	
	12	952	75.0	

Array: aaf1

Measured result are shown in Table 7.4. The coolant heat rate was calculated using an energy balance and the known coolant inlet and outlet temperatures and flow rate. The condensation rate was not measured for the Oconee coil.

Table 7.4 AAF Test Coolant Outlet Conditions.

M*

Plant	Run	Coolant Outlet	Coolant Heat Rate	Vapor Outlet	Condensation Rate
		F	$\frac{Btu}{s}$	F	$\frac{lbm}{s}$
PAL	1	116.0	454	140.0	0.392
	2	140.0	1129	208.0	1.050
	3	163.5	1770	260.0	1.750
FTC	4	139.5	390	166.0	0.355
	5	170.0	992	231.0	0.975
	6	201.0	1555	280.0	1.717
TMI	7	120.0	286	142.0	0.253
	8	166.0	651	220.0	0.633
	9	204.5	944	266.0	0.967
OCO	10	99.5	395	156.0	
	11	127.0	832	229.0	
	12	157.0	1301	277.0	

Array: aaf2

The GOTHIC results for the test series are shown in Table 7.5.

Table 7.5 GOTHIC Predictions for Fan Cooler Tests.

M*

Plant	Run	Coolant Heat Rate	Condensate Rate	Vapor Outlet	Coolant Outlet
		Btu / s	lbm / s	F	F
PAL	1	432	0.401	143.8	115.3
	2	1124	1.101	216.4	139.9
	3	1733	1.752	266.6	162.3
FTC	4	399	0.378	167.3	140.0
	5	1036	1.032	231.8	172.3
	6	1635	1.687	281.4	205.1
TMI	7	277	0.258	151.2	119.1
	8	609	0.598	225.9	161.0
	9	861	0.867	267.8	194.3
OCO	10	405	0.374	156.3	100.2
	11	871	0.853	229.8	129.6
	12	1292	1.309	278.1	156.6
Array: g					

Results are compared graphically in the following three figures. Temperatures for the three cases for each coil were similar between tests. To separate the results so that predictions and data for each coil could be clearly displayed, a temperature offset was added to each set of data and predictions in Figure 7.3. Generally good agreement between measured and predicted vapor outlet temperatures, along with close prediction of the total heat rate, indicates that the predicted split between sensible and latent heat loss from the vapor is good.

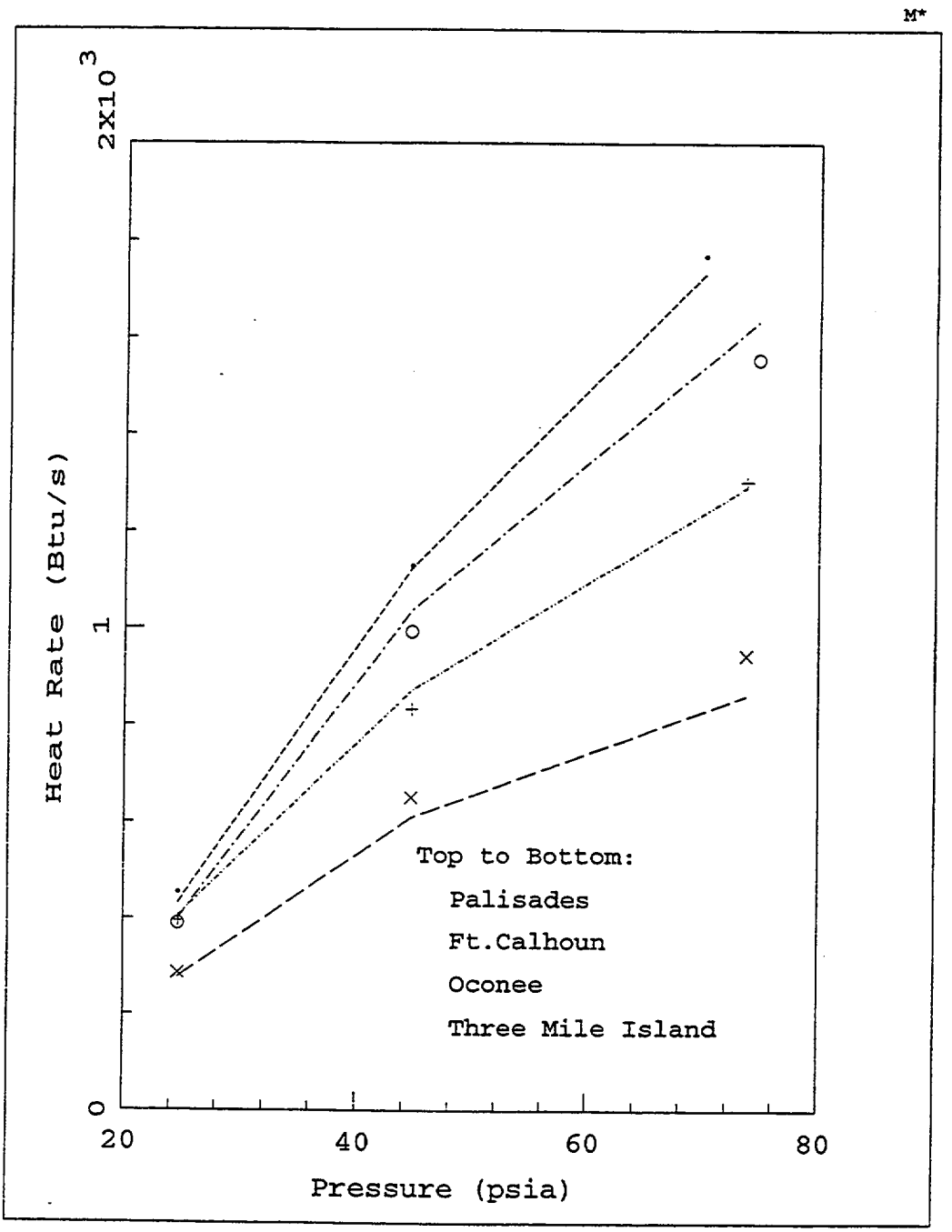

Figure 7.1 Coolant Heat Rate versus Pressure.

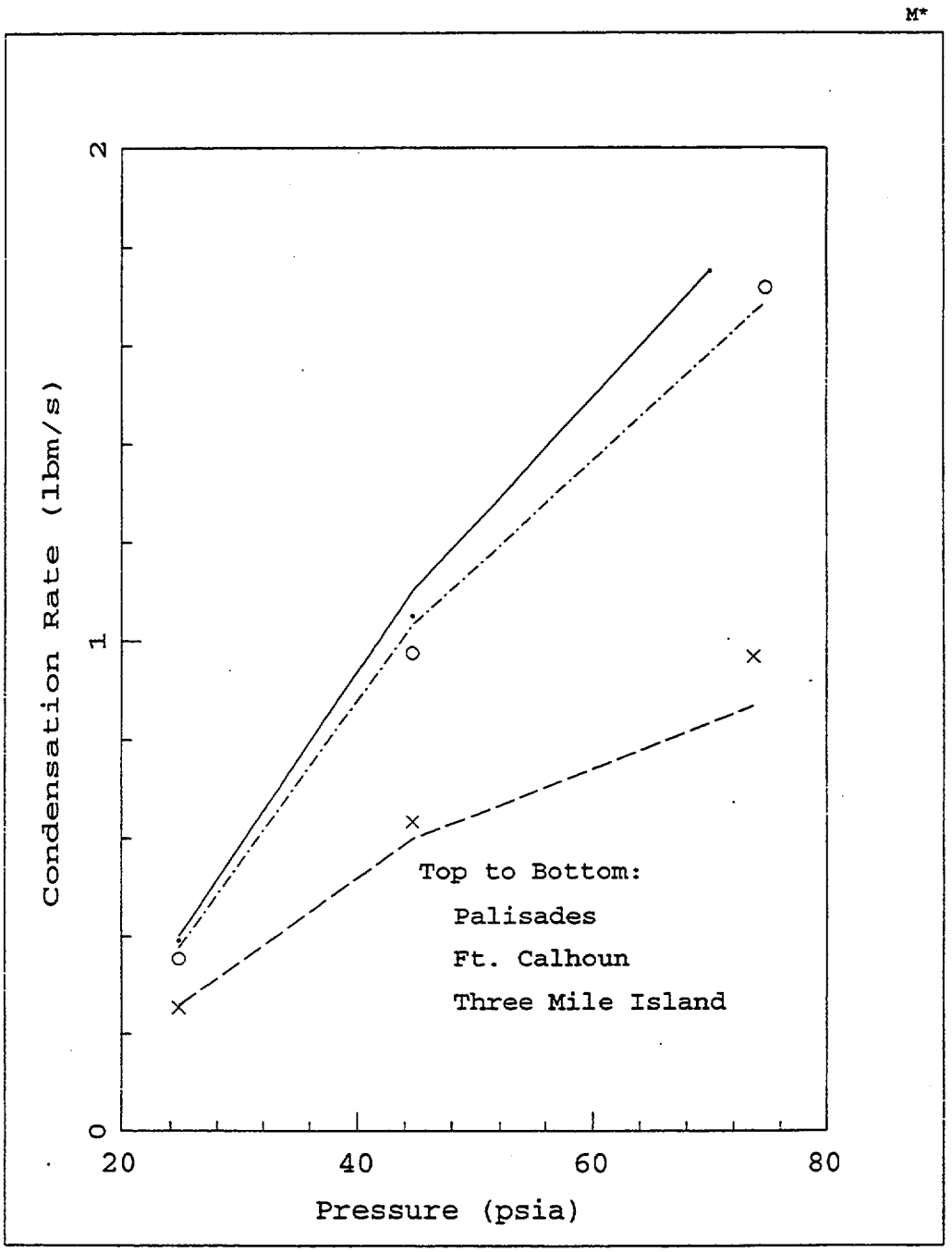

Figure 7.2 Condensation Rate versus Pressure.

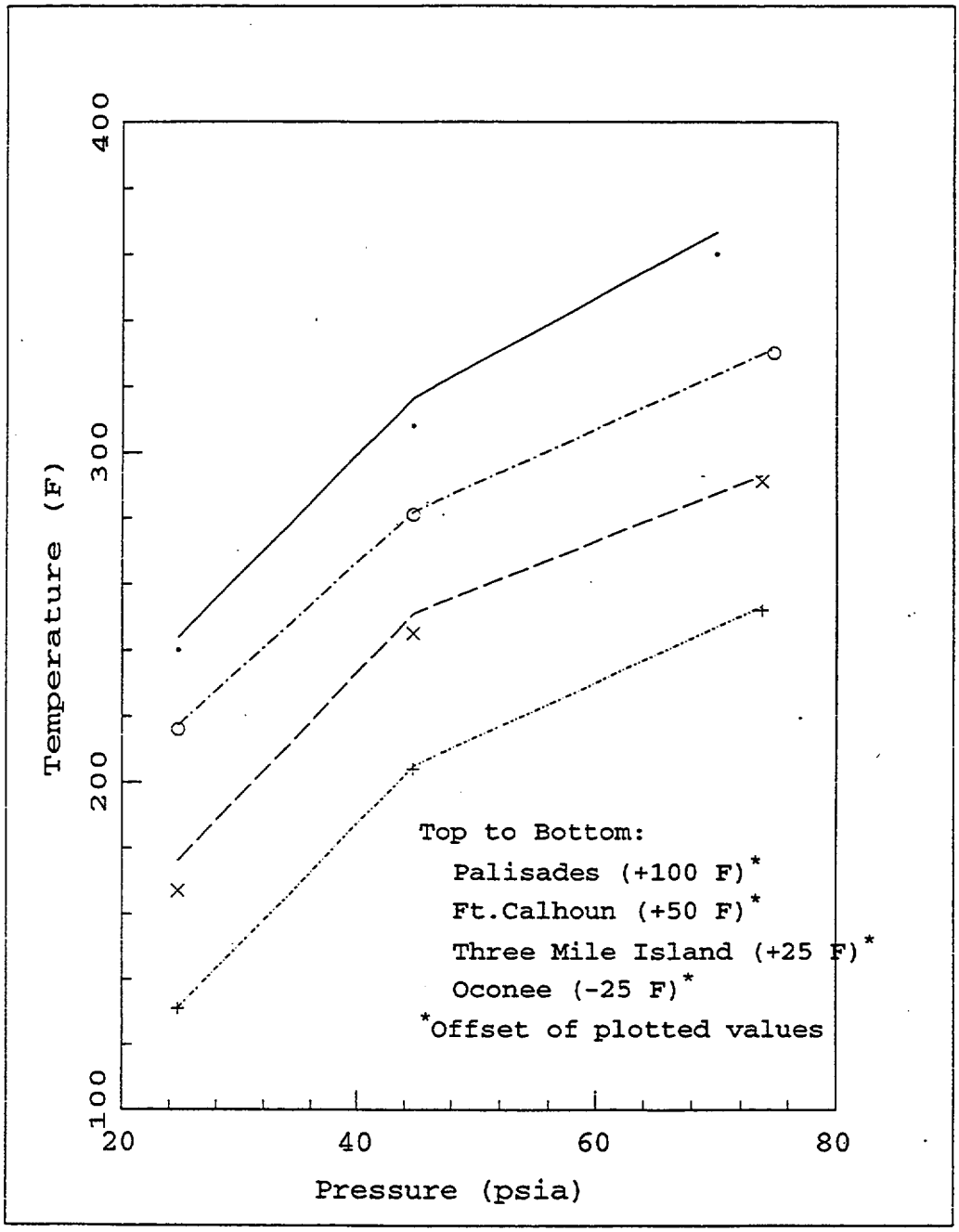

Figure 7.3 Vapor Outlet Temperature versus Pressure.

The percentage error between the measured and calculated values are shown in the table below. The test report did not give any indication of the uncertainty in the measured data nor was there any indication that more than one test

at particular test conditions were run. GOTHIC results for heat to the coolant are all within 9% of the measured values and within the reported error for the heat transfer coefficient correlations used.

Table 7.6 Percentage Variation Between GOTHIC Predictions and Measured Data for Fan Cooler Tests.

Plant	Run	Coolant Heat Rate	Condensate Rate
PAL	1	4.91	-2.30
	2	0.43	-4.86
	3	2.06	-0.11
FTC	4	-2.31	-6.48
	5	-4.47	-5.85
	6	-5.13	1.75
TMI	7	3.09	-1.98
	8	6.41	5.53
	9	8.80	10.34
OCO	10	-2.46	
	11	-4.69	
	12	0.70	

These tests cover a range of Reynolds number from 2700 to 15000. During the fan coast down, the heat exchanger Reynolds number may drop a little below 2700 (down to the 2200 range). However, the bases for the selected heat and mass transfer correlation set extend below the anticipated range. The correlation for the film thickness (Eqn 4.3) has not been tested outside the Reynolds number range for the AAF experiments but it provides reasonable values for film thickness at lower Reynolds numbers and the anticipated conditions are only slightly outside of the test range. Additional test data at lower air/steam flow rates are recommended to confirm the correlation set and the model as a whole.

7.2. Natural Convection Inside the Tubes

Two correlations were presented for calculating the natural convection inside a cylinder. The two correlations are compared with the correlation set used in GOTHIC in the Figure below for typical tube dimensions and materials (copper).

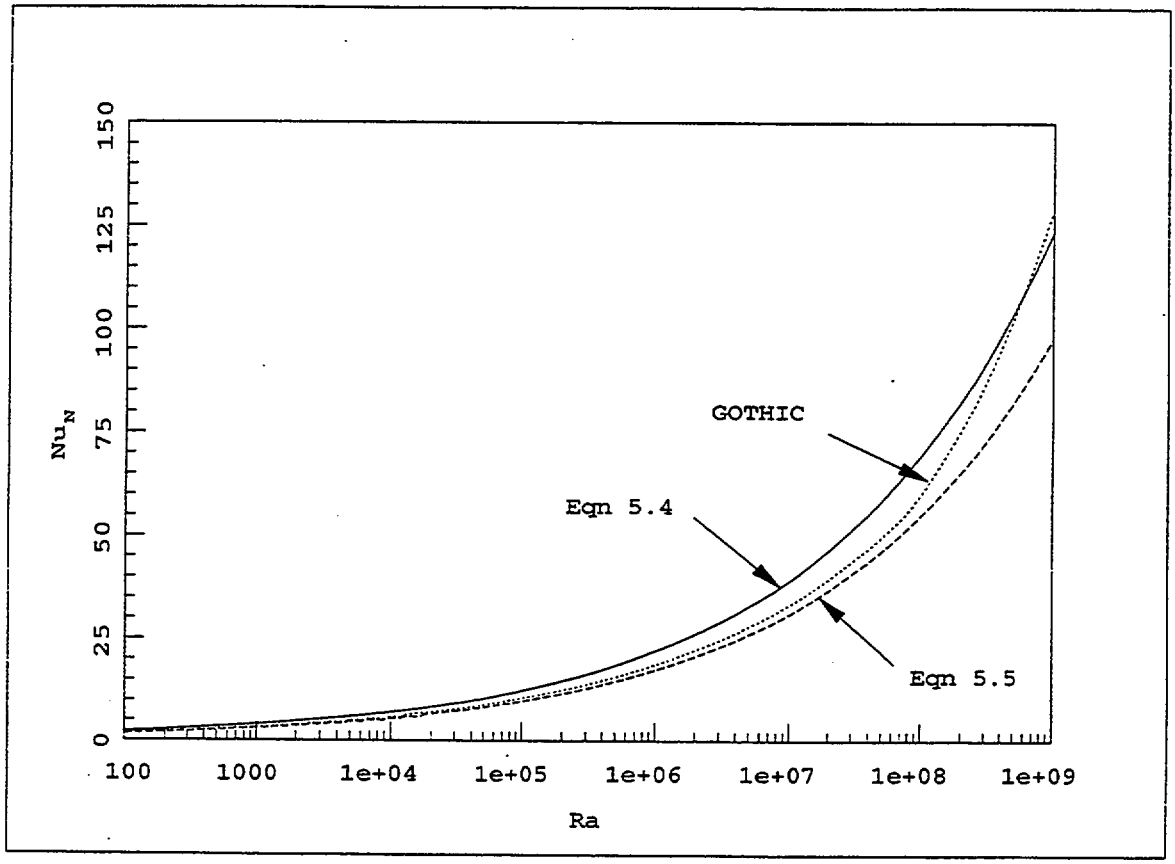

Figure 7.4 Comparison of Equations 5.3 and 5.4 with GOTHIC

When the film heat transfer option is selected in GOTHIC, which is required to get the boiling heat transfer, the correlation set used for natural convection is for heat transfer to or from a vertical plate or cylinder. At a Rayleigh number of about $1x10^8$, a turbulent natural convection correlation is used in GOTHIC, accounting for

the more rapid increase in Nu with $Ra>10^8$. For this particular application the Rayleigh number is not expected to exceed 10^7. The Nusselt numbers from the three correlations differ by about 20% with the correlation used in GOTHIC falling in between the other two.

7.3. Forced Convection

The correlations used in GOTHIC for forced convection are the same as the those recommended in this note.

7.4. Boiling Heat Transfer

For boiling heat transfer, GOTHIC uses the Chen model as described above with extensions to make it applicable to subcooled boiling. The Chen model is also used for pool boiling. The graph below compares Equation 5.11 with the GOTHIC predicted heat transfer coefficient for the inside surface of a CAC tube during LOCA with LOOP. (See the following section for a description of the model.) At about 12 seconds, the wall temperature reaches the saturation temperature and subcooled nucleate boiling begins. At about 18 seconds the liquid temperature reaches the saturation temperature and bulk boiling continues. Using the wall super heat calculated by GOTHIC, the pool boiling correlation (Equation 5.11) can be compared with the GOTHIC results for this time period. Beyond 18 seconds, the vapor volume fraction becomes large and the pool boiling model no longer applies but the Chen model can still be used. The heat transfer coefficient predicted by the Chen correlation through the tube voiding is also shown in the graph.

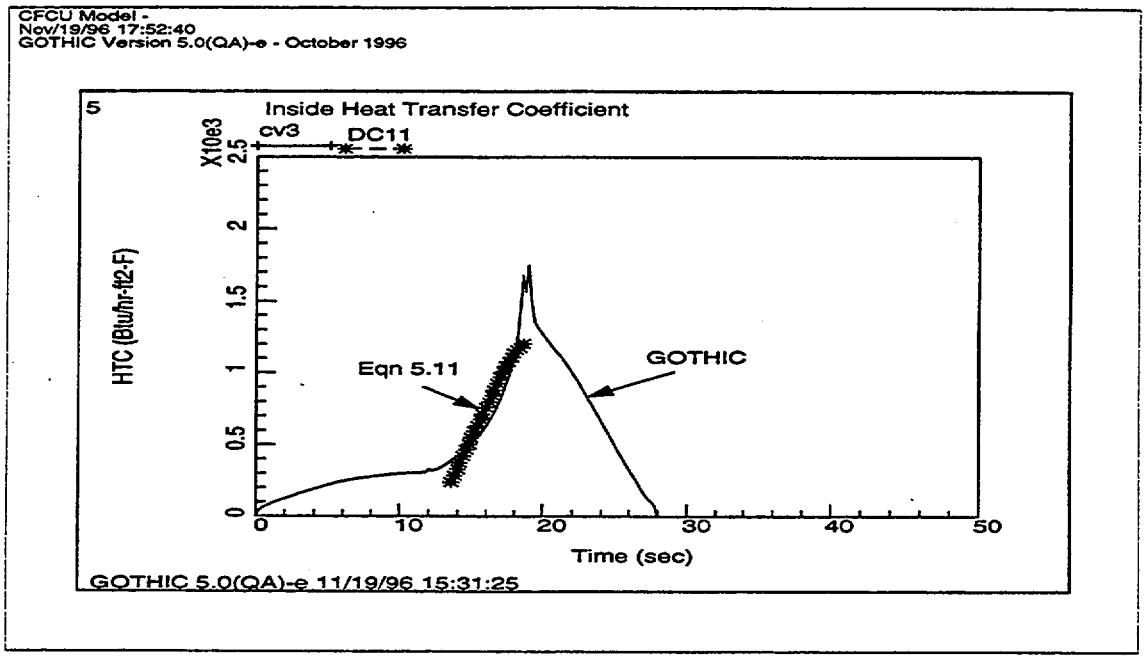

Figure 7.5 Comparison of GOTHIC and Equation 5.11 for Pool Boiling

8. GOTHIC MODELING APPROACH FOR CAC PERFORMANCE DURING LOCA WITH LOOP

As shown in the previous section, GOTHIC gives good results for the CAC heat transfer and uses correlations that have been determined applicable for the tube interior heat transfer. In this section some guidelines are presented for modeling the CAC during LOCA with LOOP.

The GOTHIC CAC model assumes quasi steady conditions, i.e., the heat transfer at any point in time is calculated assuming that the CAC reaches steady state conditions for the given primary and secondary side inlet conditions. Under this assumption, it does not consider the thermal inertia of the tubes and the water on the secondary side. For this reason it cannot be applied directly to the transient analysis for the heat up of the water in the tubes. It can, however, be relied on to provide the heat transfer rate given the water temperature and heat transfer

coefficient at the inner surface of the tube. This approach has been used to predict the onset of boiling in a CAC.

8.1. Predicting the Onset of Boiling

To predict the onset of boiling it is not necessary to model the entire secondary system. The simple model shown in the figure below will suffice. The amount of steam generated will not necessarily be correct because, as previously discussed, that depends on the dynamics of the entire secondary system.

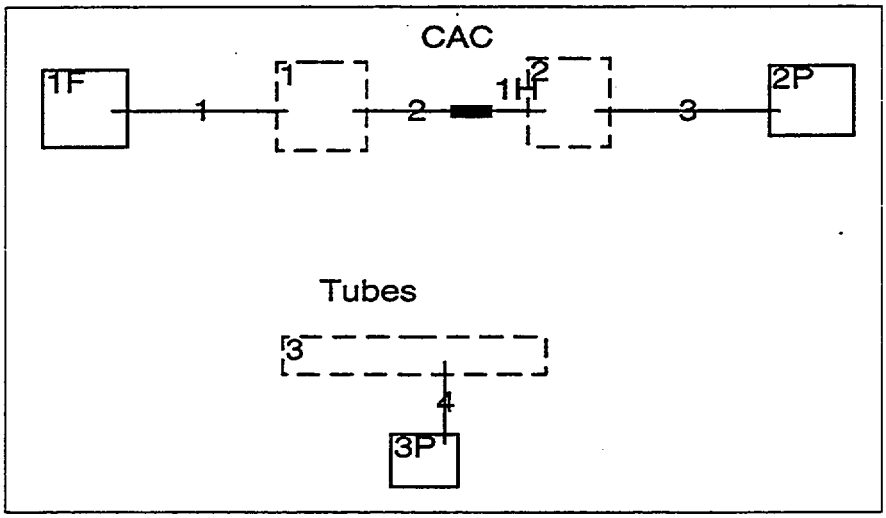

Figure 8.1 GOTHIC Noding Diagram for Onset of Boiling Calculations

In the figure above, the upper chain of volumes and flow connectors is used to represent the containment conditions and the flow through the CAC (heat exchanger 1H). The lower part of the diagram (dashed box for volume 3 and pressure boundary condition 3P) represents the water in the tubes. Control variables are used to pass the calculated heat rate from the CAC to the outer surface of a tube conductor. The inner surface of the tube conductor is connected to the water volume. Control variables are also

used to pass back to the CAC the water temperature in the tubes and the heat transfer coefficient between the water and tube surface.

The above model was run for a typical CAC operating with the fan flow coasting down as shown in Figure 8.2 and the containment temperature and pressure following the curves shown in Figures 8.3 and 8.4.

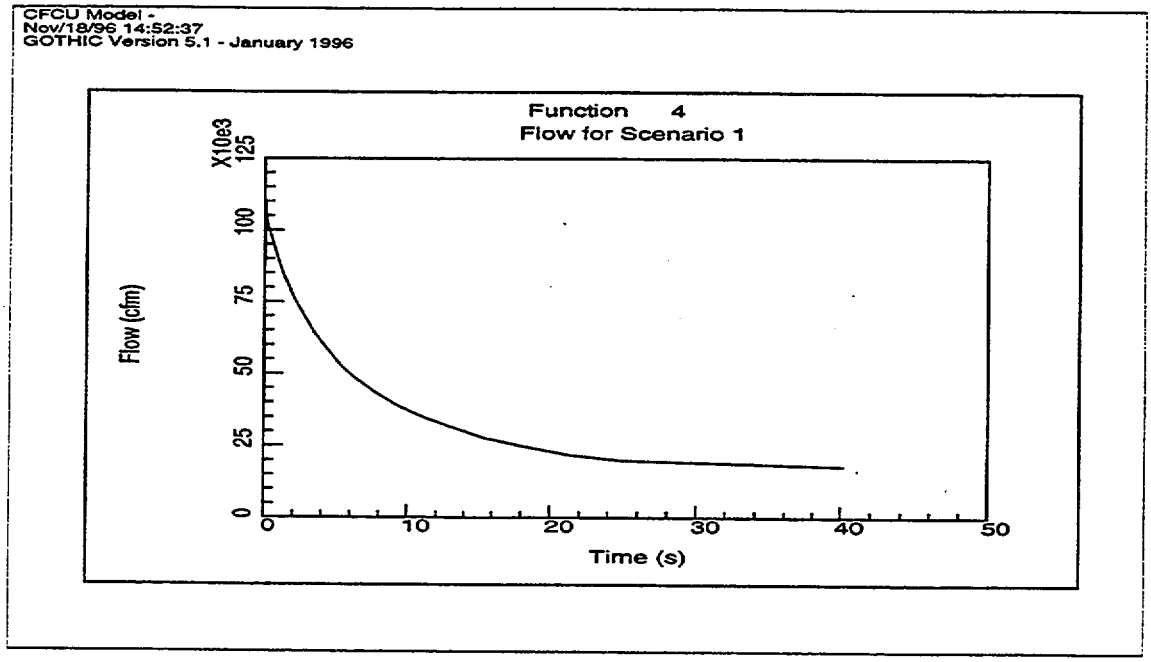

Figure 8.2 Typical Fan Coast Down Curve

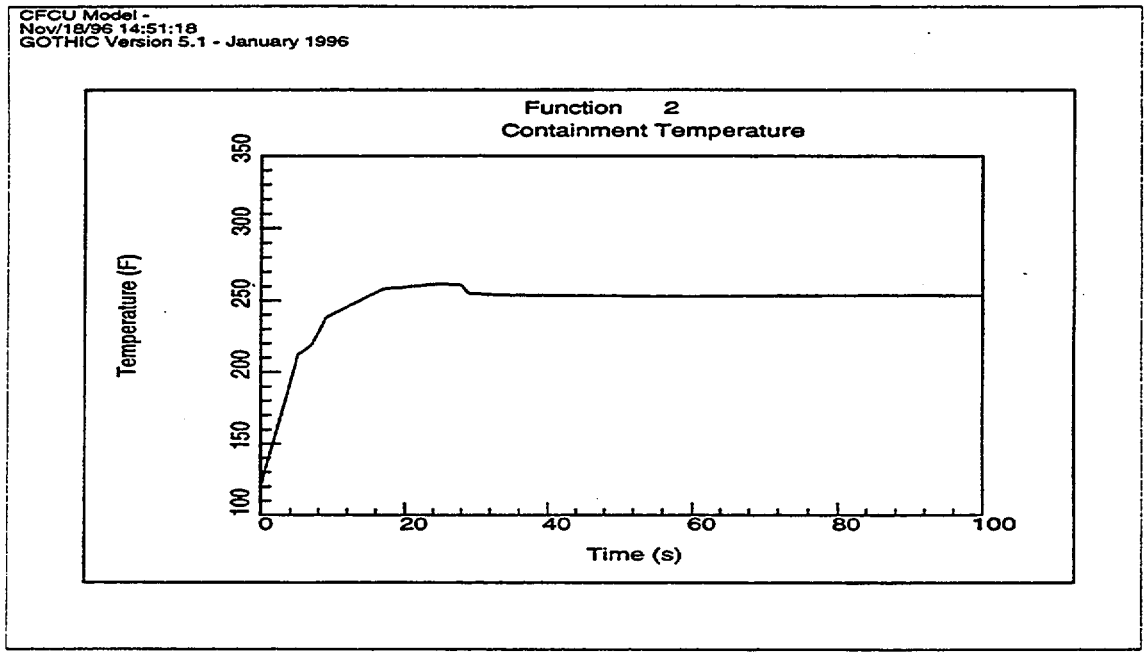

Figure 8.3 Typical Containment Temperature for LOCA

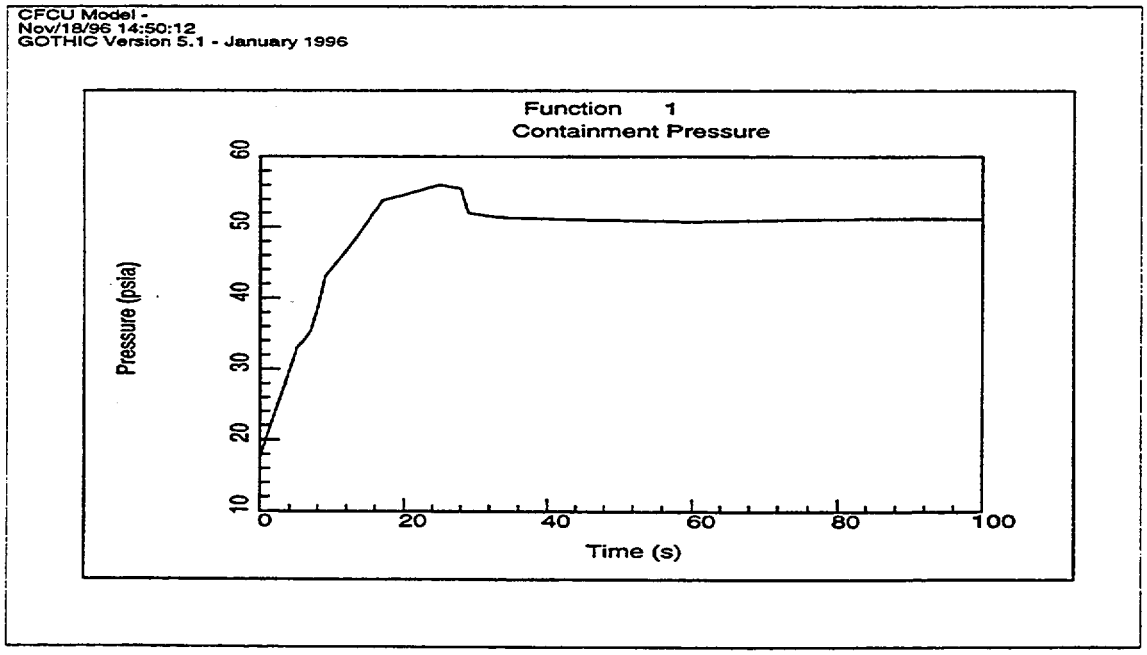

Figure 8.4 Typical Containment Pressure for LOCA

The initial temperature of the water in the tube was assumed to be 80F. The pressure in the tubes could be controlled by adjusting the pressure in boundary condition 3P. A series of runs was made to calculate the time to boil (defined as the time that the vapor volume fraction in the tubes reaches 0.1) as a function of the tube pressure. Results are shown in Figure 8.5

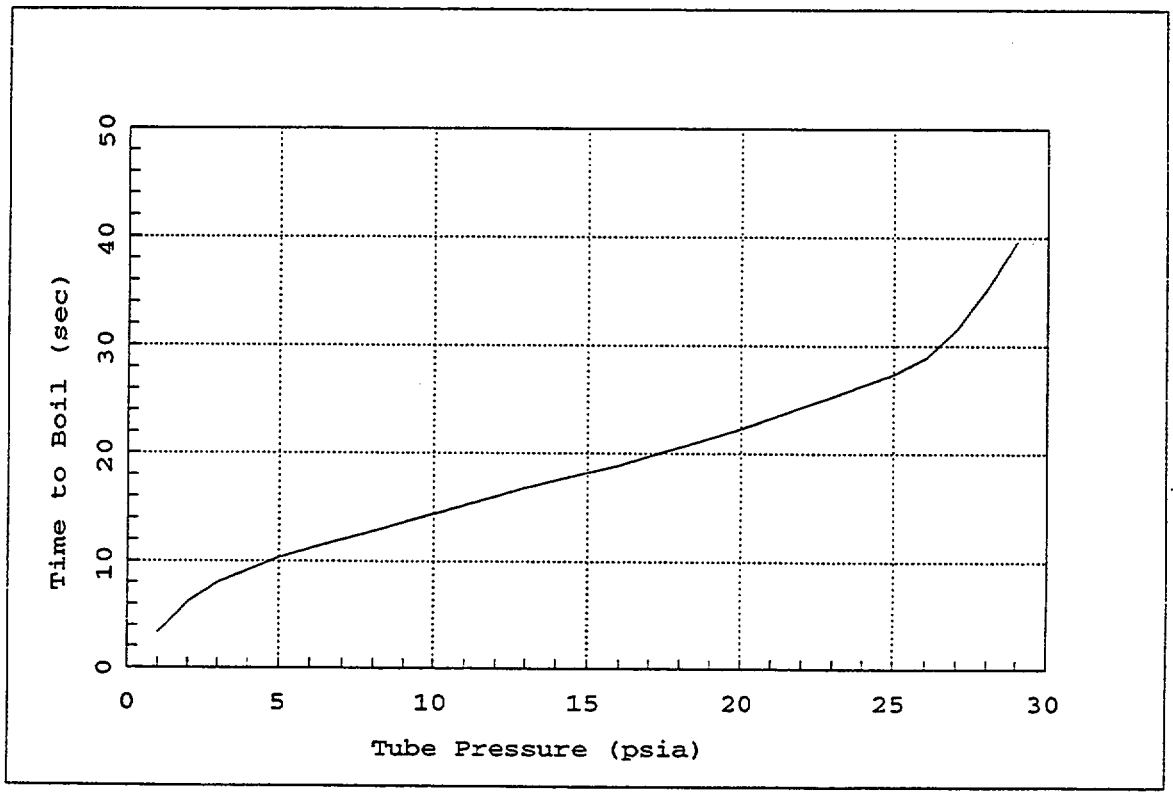

Figure 8.5 Time to Boil Curve for Typical CAC Operation During LOCA with LOOP.

8.2. Predicting Steam Region Size and Location

As previously discussed, the ultimate size and location of the steam filled regions depends not only on the heat transfer in the CAC but the dynamics of the entire secondary system. Some work has been done to investigate

the effect of various modeling approaches for the secondary system on the ultimate size of the steam region. The investigation was done using the much simplified secondary system shown in the GOTHIC noding diagram below.

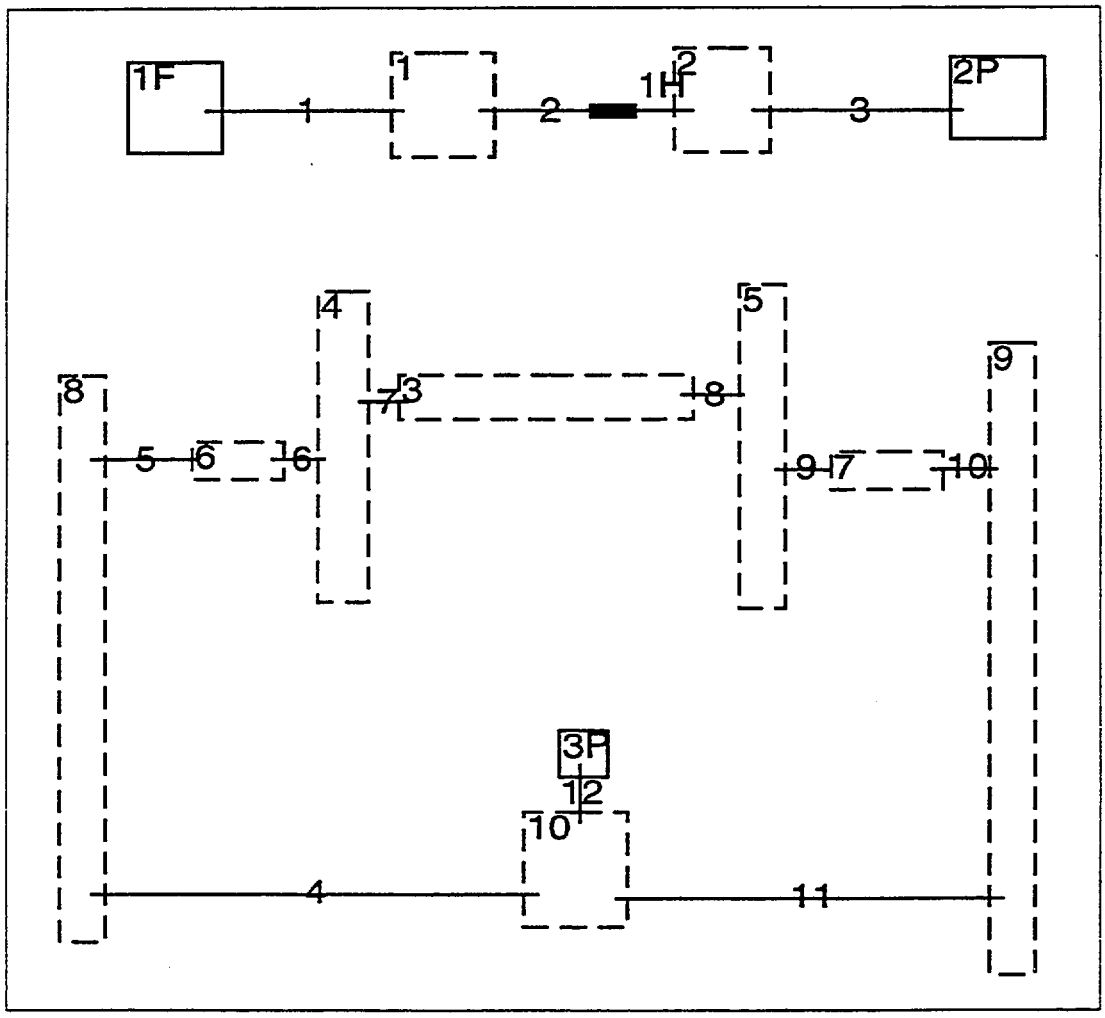

Figure 8.6 Simplified Model for Secondary System

As in the model for predicting the onset of boiling, the upper train of volumes is used to model the transient conditions in the containment, the flow through the CAC and the heat transfer to the water in the tubes. In the lower loop of volumes and junctions, volume 3 represents the CAC tubes, volumes 4 and 5 represent the inlet and outlet CAC manifolds, volumes 6 and 7 represent the pipe connections

between the manifolds and the supply and return lines represented by volumes 8 and 9. Volume 10 represents a surge tank. In this case it is assumed that the surge tank is open to the atmosphere represented by the boundary condition 3P. Control variables are used to couple the CAC model with the tube and piping model as in the onset of boiling model. This particular noding is not representative of any plant configuration but includes most of the elements found in a secondary system. In this example, the total piping volume and loss factor for the inlet side of the CAC (from the surge tank to the CAC) was much larger than the corresponding piping and volume on the outlet side to provide some asymmetry to the model as might be found in an actual plant.

A series of runs were made with variations on the above noding scheme. The cases are summarized in the table below.

Table 8.1 Cases for Secondary System Modeling Approach

Case	Description
1a	Lumped noding as shown in Figure 8.6
1b	Same as 1a except inlet and outlet manifolds were subdivided (5Hx2Wx1D).
2a	Same as 1a except 1D subdivision (3 volumes) was used for the tube volume. The initial temperature in the tube subvolumes was 70F, 80F, 90F.
3a	Same as 1a except the tube volume was split into three parallel tube volumes representing the upper, middle and lower third of the CAC.
3b	Same as 3a except the inlet and outlet manifolds were modeled as in 1b.

The noding diagrams and results for each of these test cases is given in Appendix A. All of the models predict voiding of the tubes at about the same time and rate. The models with multiple volumes for the tubes showed some variation in the time to the onset of boiling but all tube volumes entered bulk boiling within a time span of about 4 seconds. All of the models except for 2a, showed a partial or total collapse of the steam region in the tubes within 10 seconds of the initial voiding. All of the models showed some voiding of the inlet and outlet manifolds. The models with the single volume manifolds showed voiding up to 80%. This apparent limit value is an artifact of the pool geometry model assumed in GOTHIC for lumped volumes. which allows only steam to exit the volume when the water level is below the junction end elevation. With the subdivided models (1b and 3b) the manifolds are more completely filled with steam at least part of the time.

The boiling and condensation process that takes place in the tubes and the connected piping is very complex and difficult to model. Without experimental data we are left to engineering judgement regarding the best modeling approach. From the limited testing described above, it appears that it is sufficient to model the CAC with a single tube volume. If this tube volume is connected directly to a large piping volume, all of the steam leaving the tube will be condensed in the large volume and the predicted void region will be limited to the CAC tubing. Using smaller volumes around the CAC permits local heating of the water and limits the amount of condensation and, therefore, predicts larger steam filled regions and possible secondary voiding due to depressurization during the initial bubble collapse. It is recommended that at least the manifold piping be subdivided and that the subdividing should extend out beyond the region where condensation is occuring prior to pump restart. The optimum number and size of the subvolumes has not been determined but there are some practical limits imposed by the GOTHIC numerics. During the boiling process, bubbles form in the subvolumes and then rapidly collapse, leading to a local small pressure spike. The code must use small time steps to maintain a stable solution during this process.

To predict the water hammer loads it is necessary to know the size of the steam region just before it collapses. The collapse may be caused by the pump restart or because it comes into contact with some cold water. As seen in the example cases above, GOTHIC may predict total or partial collapse of the steam region before the pump restarts. However, the uncertainties in the analysis are too large to rely on the close timing of this collapse and the pump restart for estimating the water hammer potential. Instead, the maximum steam volume predicted any time before pump restart should be used to estimate water hammer loads.

8.3. Uncertainty in GOTHIC Results

Based on the data comparison of GOTHIC with the AAF data and the known accuracy of the single phase liquid heat transfer coefficient for inside the tubes and some parametric studies completed, it is estimated that GOTHIC can predict the time to boiling within 20%.

Although GOTHIC'S ability to calculate the size of the steam region is based on sound thermal-hydraulic models, it has not been compared with experimental data. Until such verification can be completed it must be accepted as a rough estimate and additional engineering judgement and conservatisms should be applied to provide a margin of safety.

9. PROPERTIES

The following are some properties and geometric information is used in calculations in this note.

$$D ::= 0.5\ \text{in} \qquad \text{tube ID} \tag{9.1}$$

$$\rho_l ::= 62.4\ \frac{\text{lbm}}{\text{ft}^3} \qquad \text{liquid density} \tag{9.2}$$

$$c_{pl} ::= 1\ \frac{\text{Btu}}{\text{lbm-R}} \qquad \text{liquid specific heat} \tag{9.3}$$

$$\mu_l ::= 150 \times 10^{-7}\ \frac{\text{lbf-s}}{\text{ft}^2} = \boxed{1.737\ \frac{\text{lbm}}{\text{hr-ft}}} \tag{9.4}$$

$$k_l ::= 0.36\ \frac{\text{Btu}}{\text{hr-R-ft}} \qquad \text{liquid conductivity} \tag{9.5}$$

$$\beta_l ::= 1.9 \times 10^{-4}\ \frac{1}{\text{R}} \qquad \text{volumetric expansion coeff.} \tag{9.6}$$

$$\frac{g \cdot \rho_1^{\,2} \cdot c_{p1} \cdot \beta_1 \cdot 1\,R \cdot D^3}{\mu_1 \cdot k_1} = \boxed{3.568\ X\ 10^{+04}} \tag{9.7}$$

$$k_t ::= 200\ \frac{Btu}{hr\text{-}R\text{-}ft} \quad \text{tube wall conductivity} \tag{9.8}$$

$$\delta_t ::= 0.05\ in \quad \text{tube wall thickness} \tag{9.9}$$

10. NOMENCLATURE

A_{fin} - fin surface area
A_{tot} - fin plus tube surface area
c_p - specific heat at constant pressure
D - hydraulic diameter
d_t - tube ID
g - gravitational acceleration
H_{eff} - effective heat transfer coefficient
H - heat transfer coefficient
H_{vi} - heat transfer coefficient for vapor to liquid/vapor interface
H_m - mass transfer coefficient
k - thermal conductivity
k_{fin} - fin thermal conductivity
k_l - liquid thermal conductivity
k_v - vapor conductivity
l - fin length
L - plate height
m - fin effectiveness parameter
M_a - air molecular weight
M_s - steam molecular weight
Nu_h - Nusselt number for heat transfer - H_hD/k
Nu_m - Nusselt number for mass transfer - $H_mD/(\chi\lambda)$
P - total pressure
P_c - critical pressure
P_r - relative pressure P/P_c
P_{sat} - saturation pressure
Pr - Prandtl number - $c_p\mu/k$
Pr_s - Prandtl number evaluated at liquid/vapor interface
Re - Reynolds number - $\rho VD/\mu$
Re_{tp} - two phase Reynolds number
S_l - tube spacing in the direction of cross flow
S_t - tube spacing transverse to the cross flow
Q'' - heat flux
Q''_{conv} - sensible heat flux
Q''_{cond} - heat flux due to condensation
T_i - liquid/vapor interface temperature
T_f - liquid film temperature

T_l - liquid temperature
T_v - vapor temperature
T_{wi} - tube inner surface temperature
T_{wo} - tube outer surface temperature
V - velocity
V_a - air molecular volume (29.9)
V_s - steam molecular volume (18.8)
X_{tt} - Martinelli factor
x - thermodynamic quality

ϕ_v - steam mole fraction in the bulk
ϕ_i - steam mole fraction at liquid/vapor interface
β - volumetric thermal expansion coefficient
δ_f - liquid film thickness
δ_{fin} - fin thickness
δ_t - tube wall thickness
Γ'' - rate of phase change per unit area
λ - binary gas diffusion coefficient
η - fin effectiveness coefficient
η_0 - fin heat transfer factor
μ - viscosity
σ - surface tension
ρ - density
ρ_l - liquid density
ρ_v - vapor density
χ - mole concentration of the bulk gas/steam mixture

11. REFERENCES

F. Kreith, "Principles of Heat Transfer", International Textbook Company, Scranton, PA, 1965.

Handbook of Single-Phase Convective Heat Transfer, John Wiley & Sons, New York, 1987.

Collier, J., "Convective Boiling and Condensation", McGraw-Hill, NY, 1981.

Bird, R.B., Stewart, W.E. and Lightfoot, E.N., "Transport Phenomena", John Wile & Sons, Inc., New York, 1960.

Holman, J.P., "Heat Transfer", McGraw-Hill, NY, 1963.

Hong, S.W., et al, "Analytical and Experimental Results for Combined Forced and Free Laminar Convection in Horizontal Tubes, Proc. 5th Int. Heat Transfer Conf., Tokyo, Vol. 3, NC4.6, 1974.

Borishanski, V.M., "Correlation of the Effect of Pressure on the Critical Heat Flux and Heat Transfer Rates Using the Theory of Thermodynamic Similarity", in Problems of Heat Transfer and Hydraulics of Two-Phase Media, ed. S.S. Kutateladze, Pergamon, Oxford, 1969.

Chen, J.C., "Correlation for Boiling Heat Transfer to Saturated Liquids in Convective Flow", Ind. Eng. Chem. Process Des. Dev., Vol. 5, 1966.

Churchill, S.W. and I.C. Brier, "Convective Heat Transfer from a Gas Stream at High Termperature to a Circular Cylinder Normal to the Flow", Chem. Eng. Prog. Symp. Ser., Vol. 51, 1955.

Kays, W.M., and R.K. Lo, "Basic Heat Transfer and Flow Friction Design Data for Gas Flow Normal to Banks of Staggered Tubes - Use of a Transient Technique:, Tech. Rep.

15, Navy Contract N6-onr-251 T. O. 6, Standford Univ., 1952.

R.D. Rivers, et al., Design and Testing of Fan Cooler-Filter Systems for Nuclear Applications, Topical Report AAF-TR-7101A, January 20, 1972, American Air Filter Company, Inc., P.O. Box 1100, Louisville, Kentucky 40201.

ASME Steam Tables, 1967.

F.P. Incropera and D.P. DeWitt, 'Fundamentals of Heat Transfer', 1981.

Kays, W.M., "Convective Heat and Mass Transfer", McGraw-Hill, NY, 1987.

"Heat Exchanger Design Handbook", Hemisphere Publishing, NY, 1989.

"Handbook of Heat Transfer Fundamentals", edited by W.M. Rohsenow, et al., McGraw-Hill, NY, 1985.

Collier, J.G., "Pool Boiling", in Heat Exchanger Design Handbook, Hemisphere Publishing, 1989.

J.A. Block, et al., "An Evaluation of PWR Steam Generator Water Hammer", NUREG-0291, June 1977.

APPENDIX A

NODING STUDIES FOR STEAM REGION GROWTH

APPENDIX A

NODING STUDIES FOR STEAM REGION GROWTH

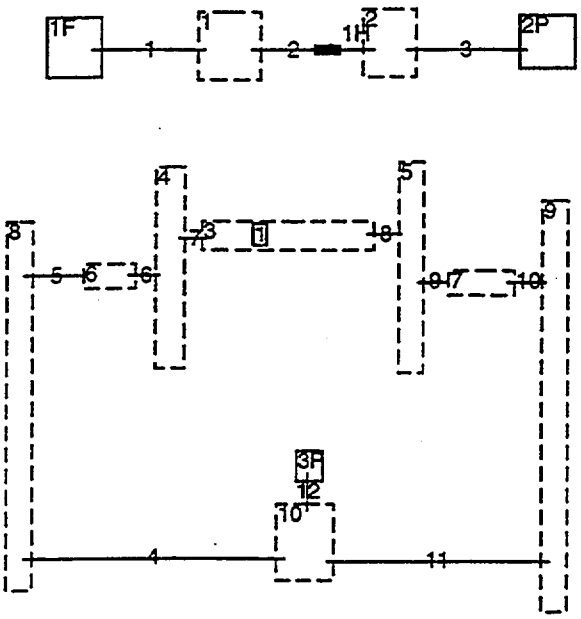

Figure A1. Simplified Loop Model - Case 1a

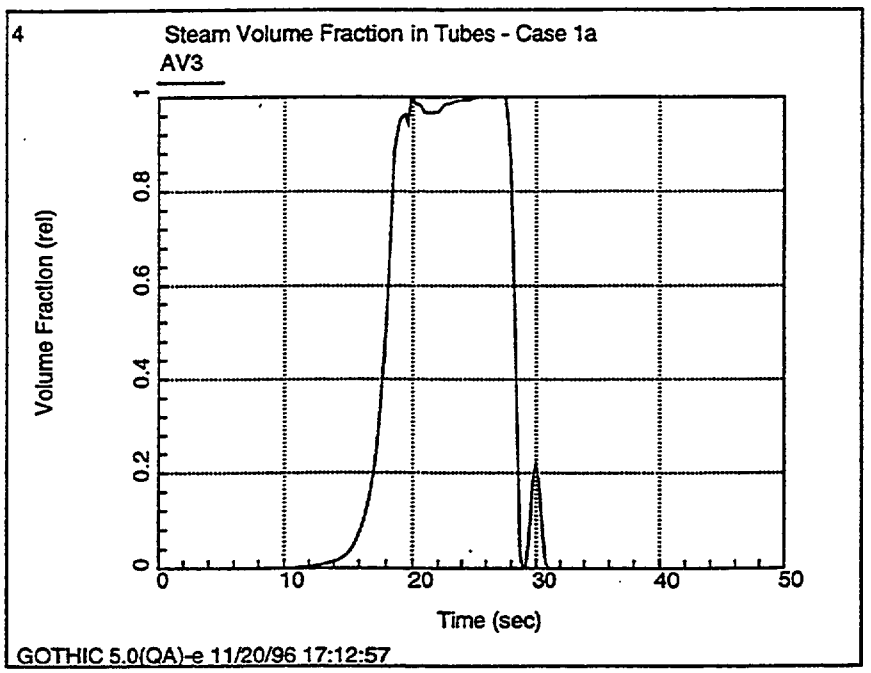

Figure A2. Steam Volume Fraction in Tubes - Case 1a

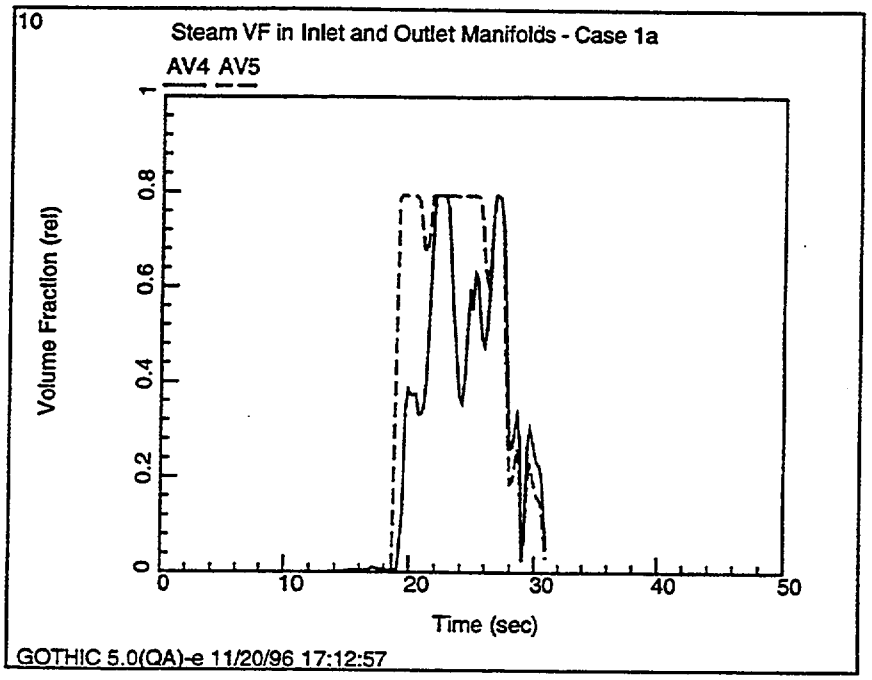

Figure A3. Steam Volume Fraction in Inlet and Outlet Manifolds - Case 1a

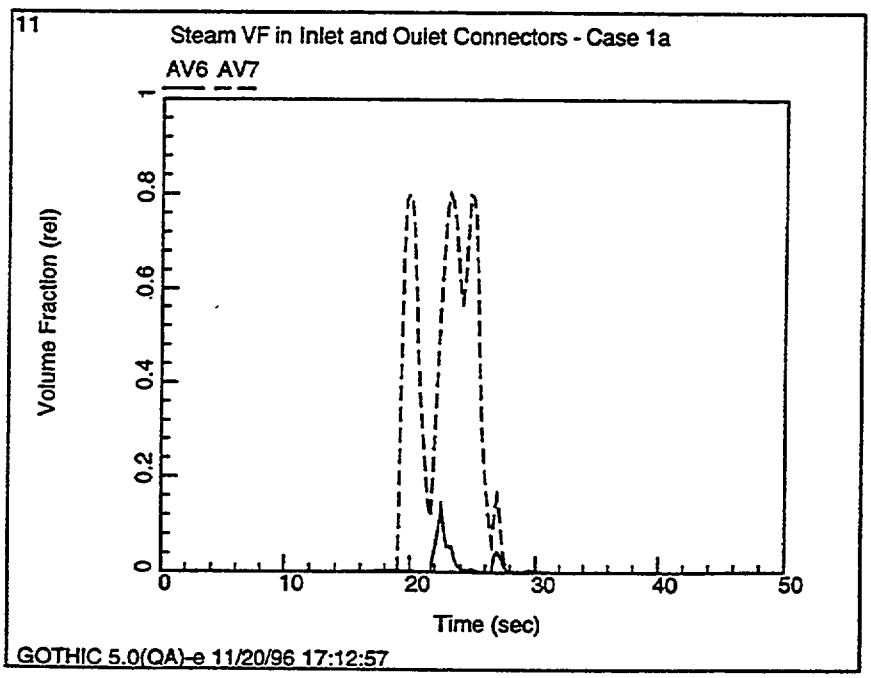

Figure A4. Steam Volume Fraction in Inlet and Outlet Connectors - Case 1a

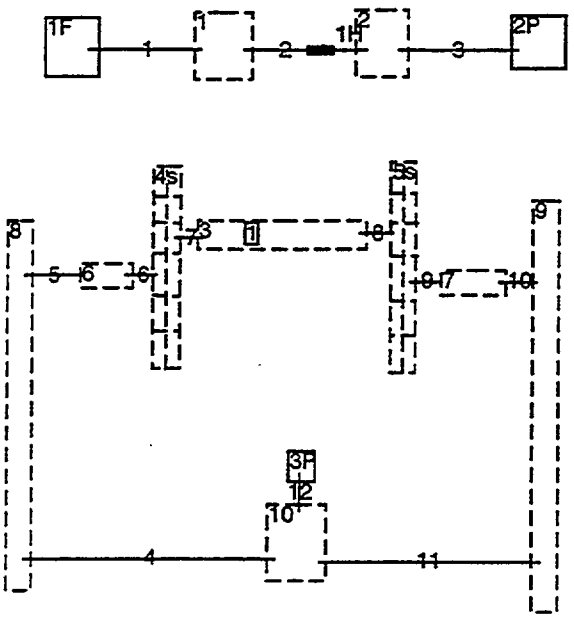

Figure A5. Simplified Loop Model - Case 1b

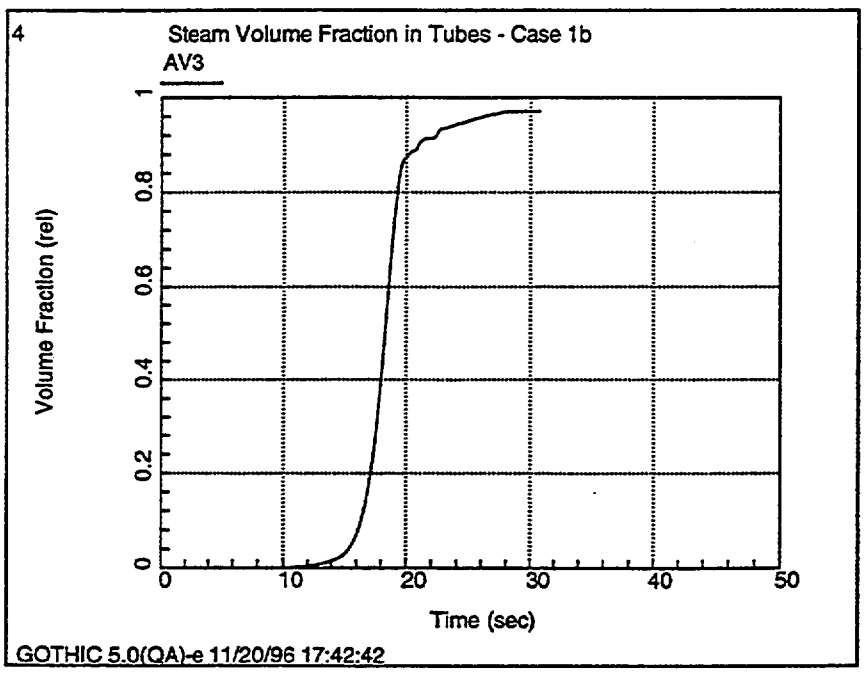

Figure A6. Steam Volume Fraction in Tubes - Case 1b

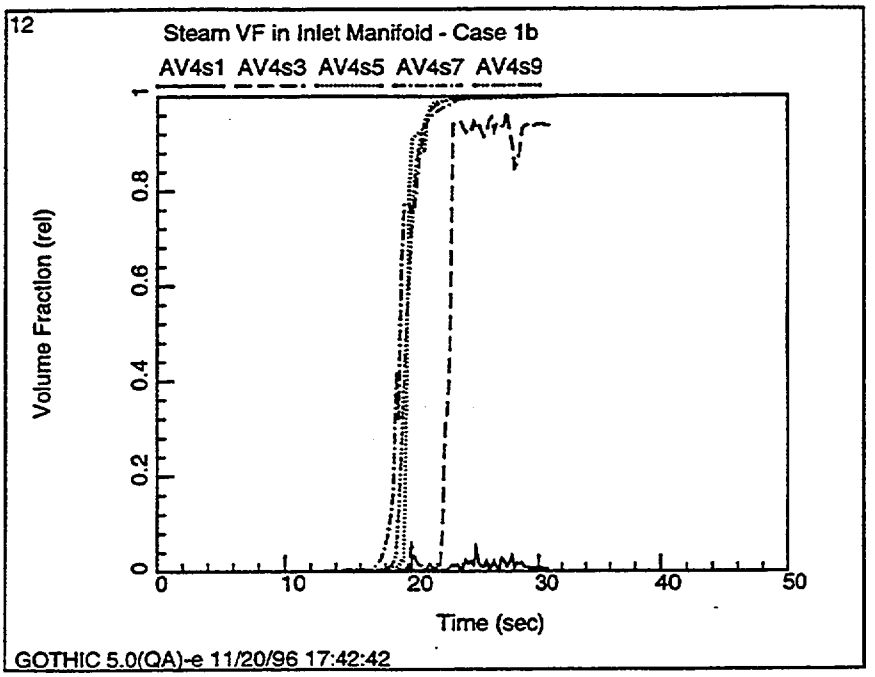

Figure A7. Steam Volume Fraction in Inlet Manifolds - Case 1b

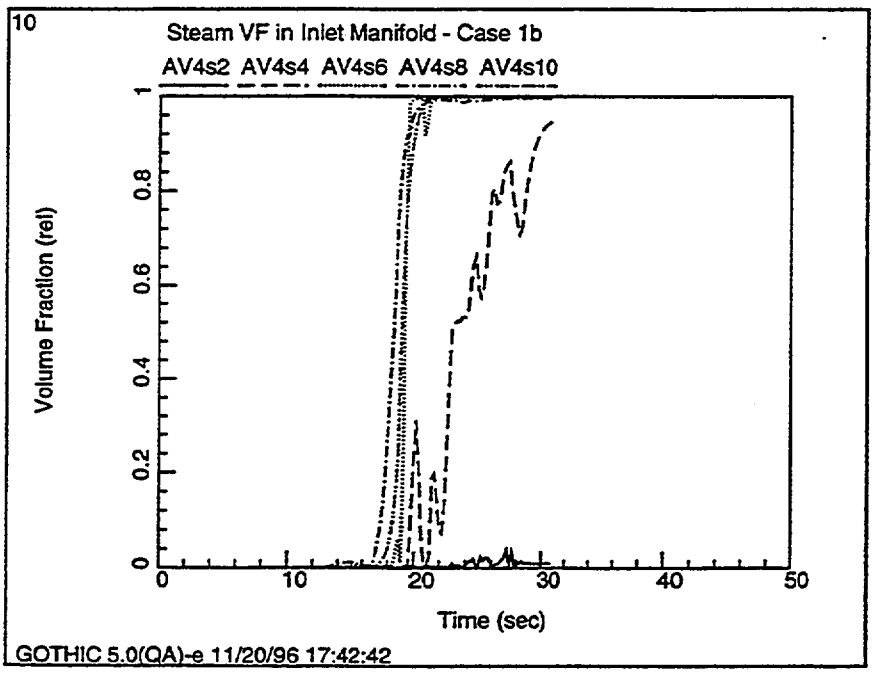

Figure A8. Steam Volume Fraction in Inlet Manifolds - Case 1b

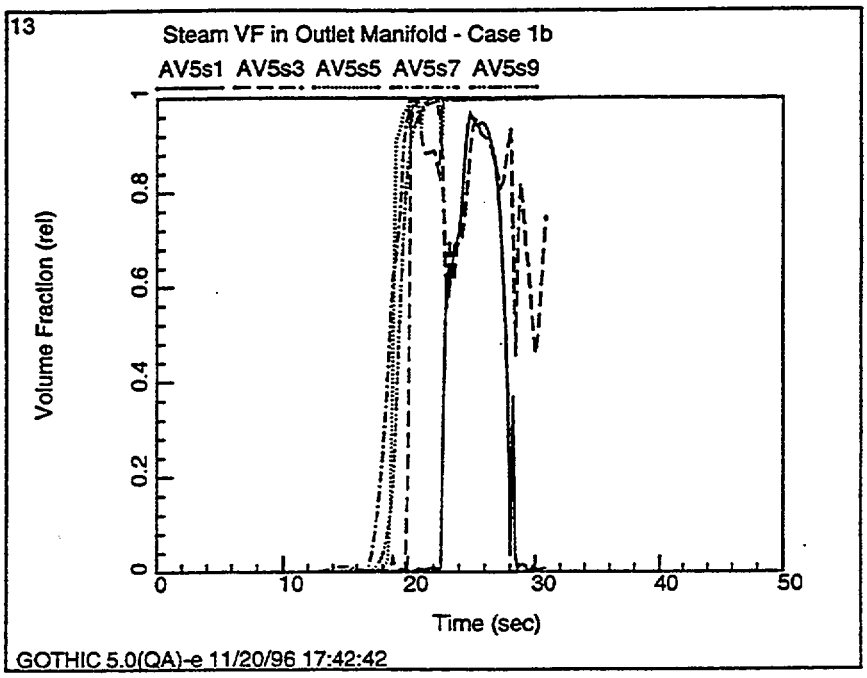

Figure A9. Steam Volume Fraction in Outlet Manifolds - Case 1b

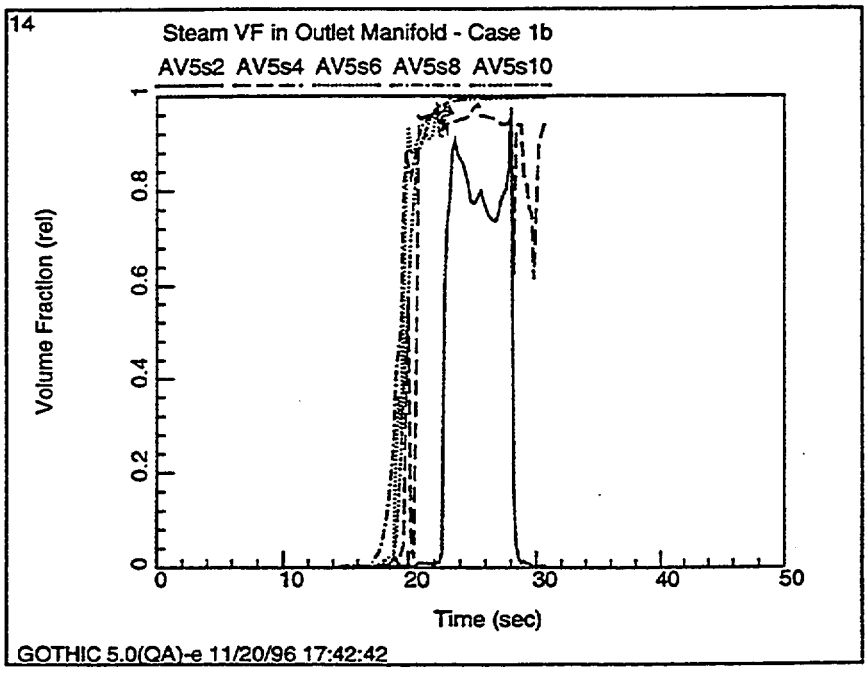

Figure A10. Steam Volume Fraction in Outlet Manifolds - Case 1b

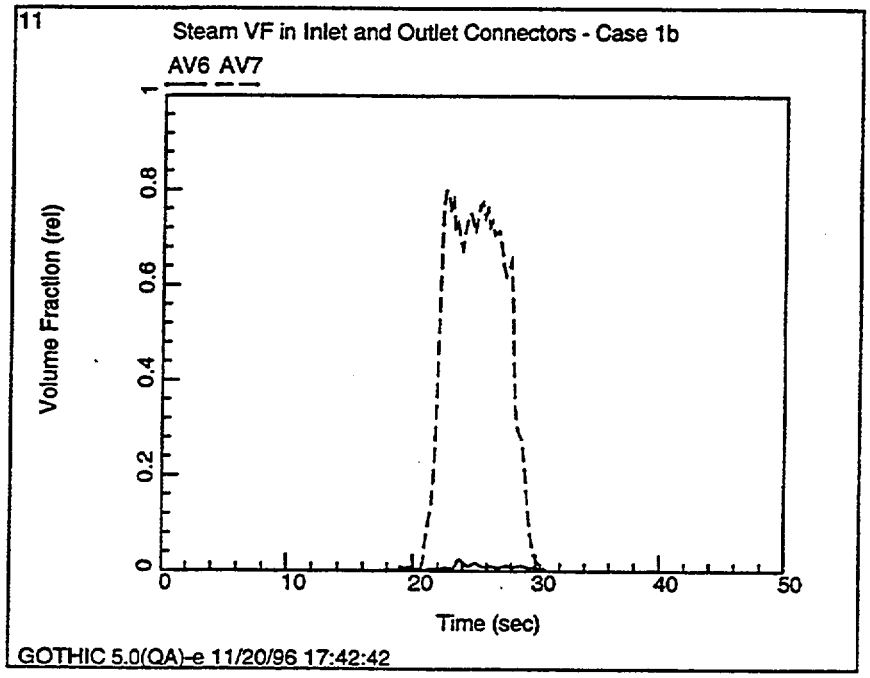

Figure A11. Steam Volume Fraction in Inlet and Outlet Connectors - Case 1b

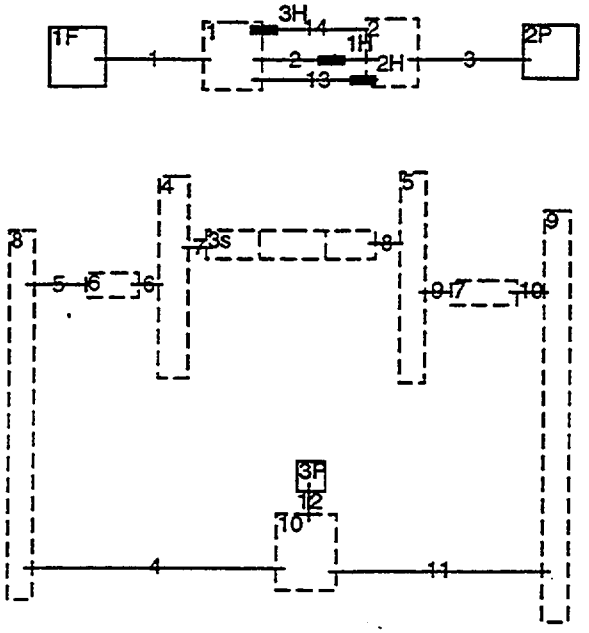

Figure A12. Simplified Loop Model - Case 2a

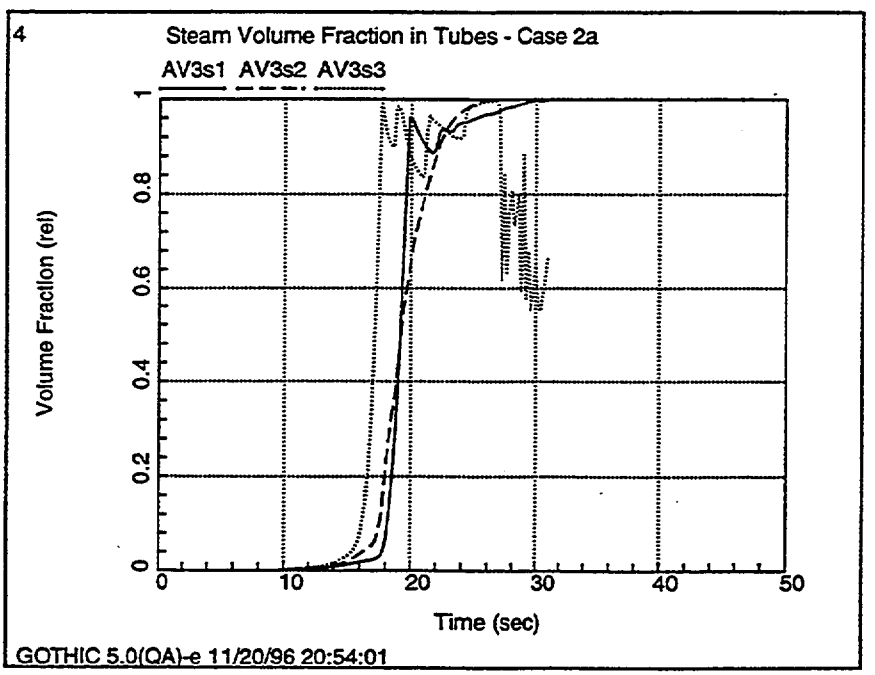

Figure A13. Steam Volume Fraction in Tubes - Case 2a

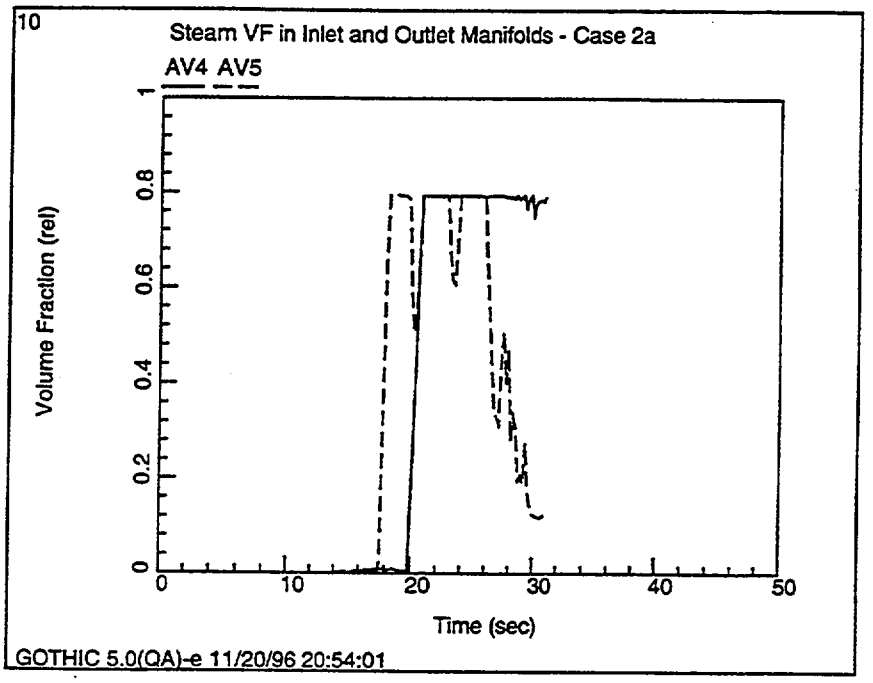

Figure A14. Steam Volume Fraction in Inlet and Outlet Manifolds - Case 2a

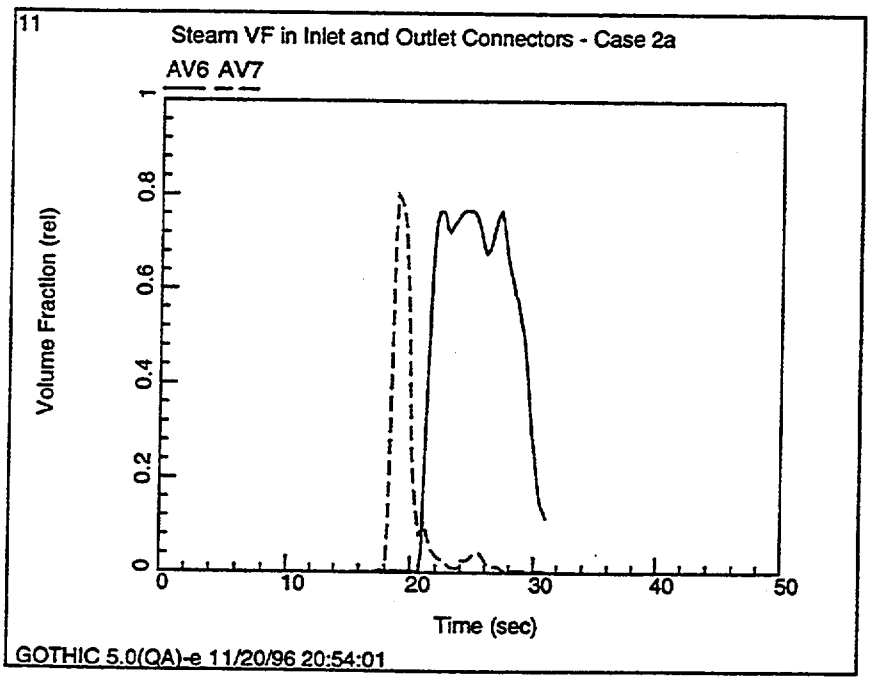

Figure A15. Steam Volume Fraction in Inlet and Outlet Connectors - Case 2a

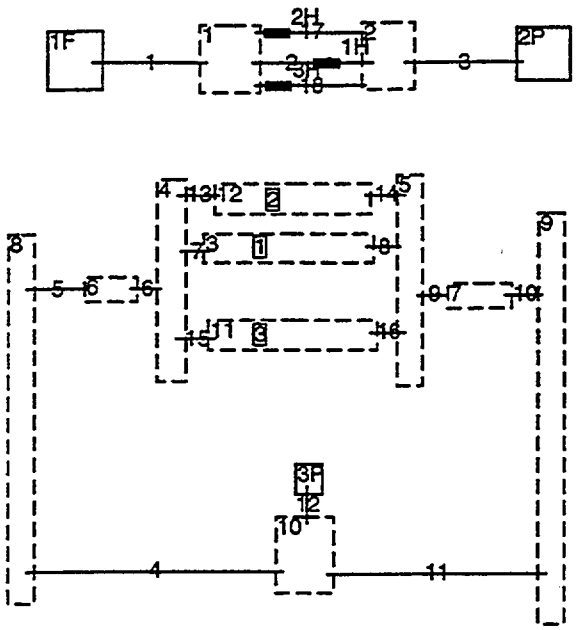

Figure A16. Simplified Loop Model - Case 3a .

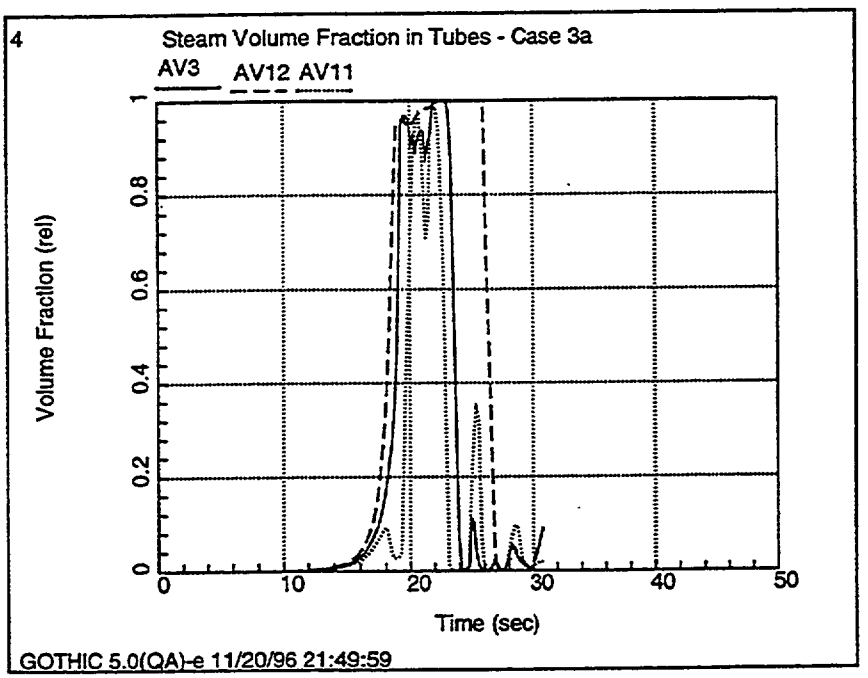

Figure A17. Steam Volume Fraction in Tubes - Case 3a

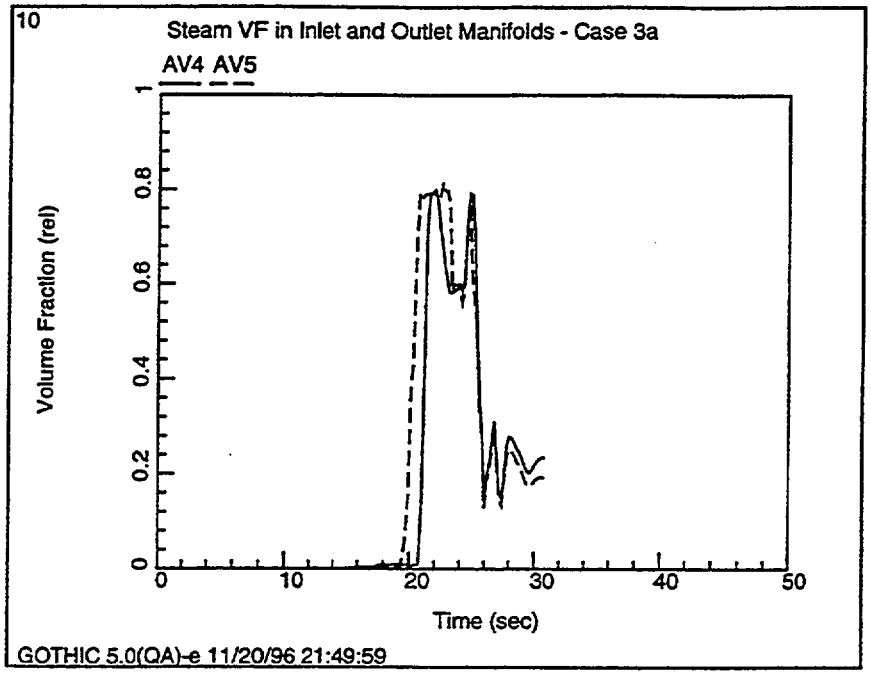

Figure A18. Steam Volume Fraction in Inlet and Outlet Manifolds - Case 3a

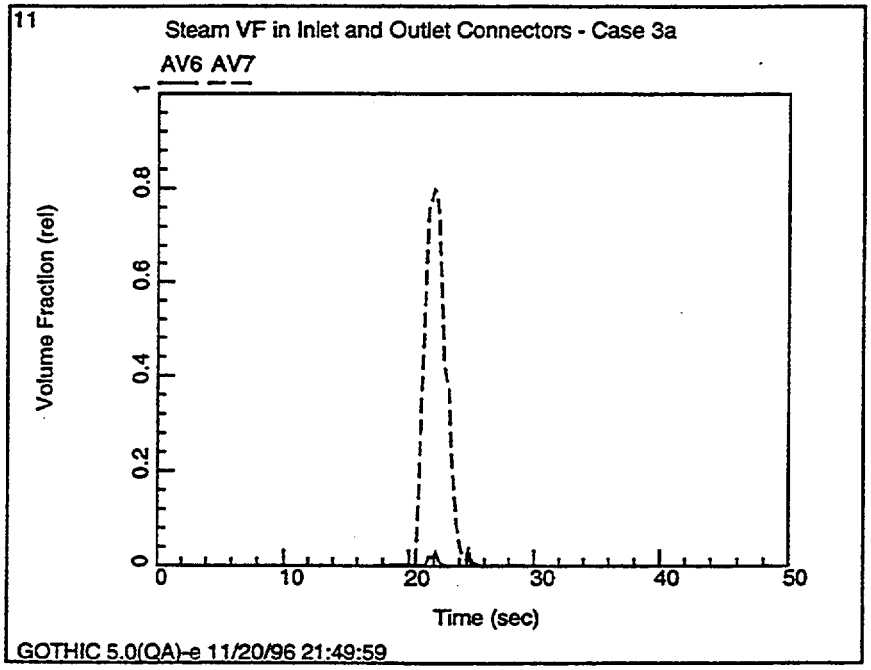

Figure A19. Steam Volume Fraction in Inlet and Outlet Connectors - Case 3a

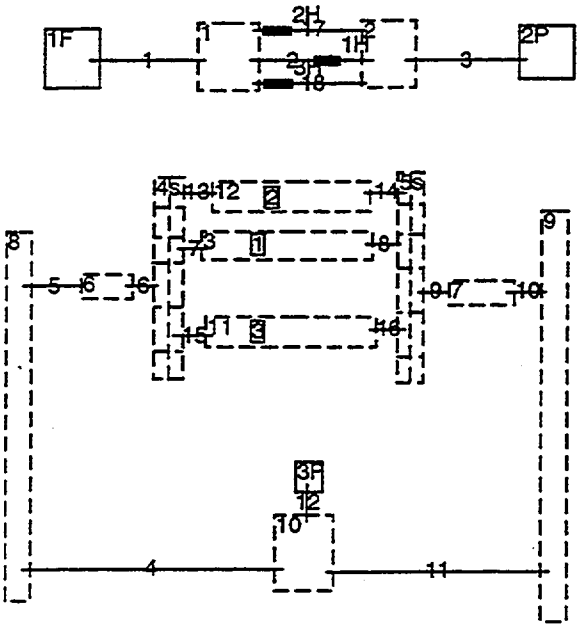

Figure A20. Simplified Loop Model - Case 3b

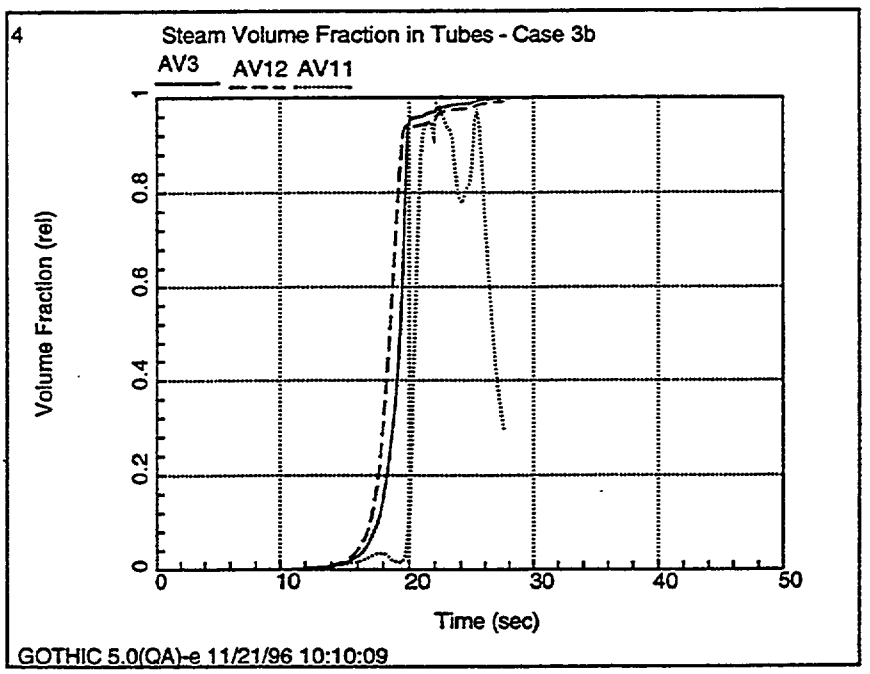

Figure A21. Steam Volume Fraction in Tubes - Case 3b

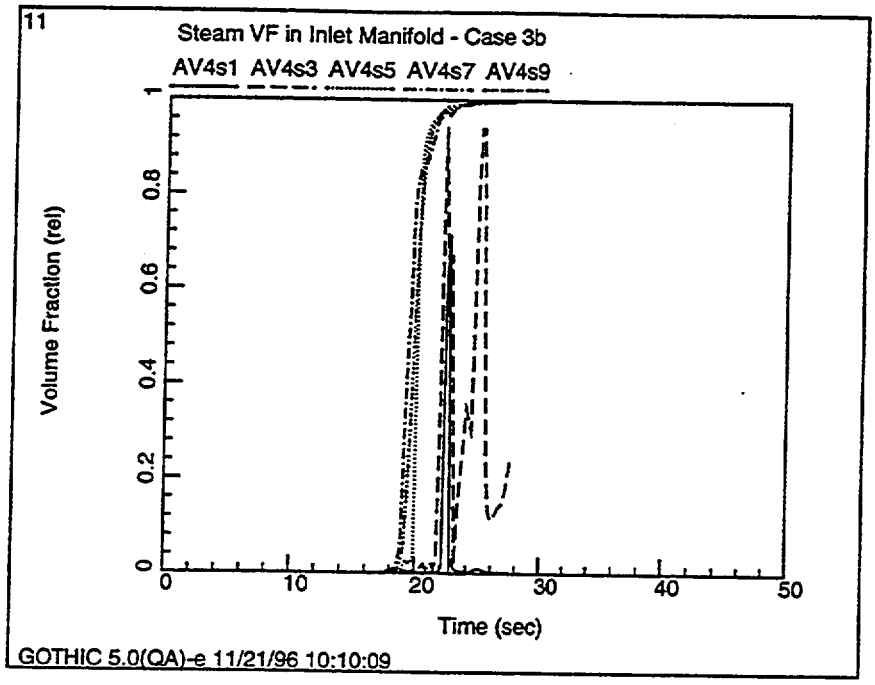

Figure A22. Steam Volume Fraction in Inlet Manifolds - Case 3b

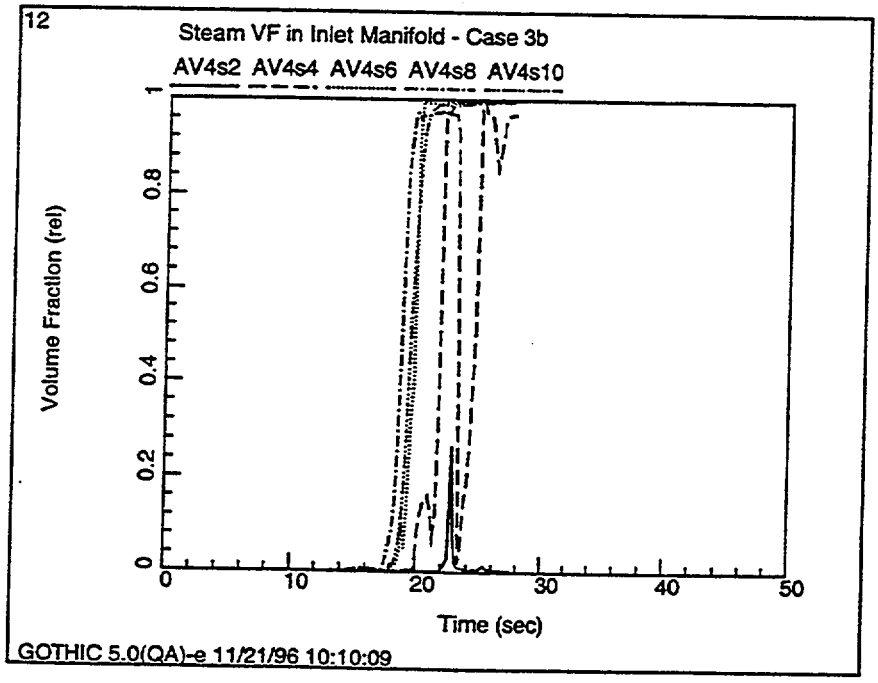

Figure A23. Steam Volume Fraction in Inlet Manifolds - Case 3b

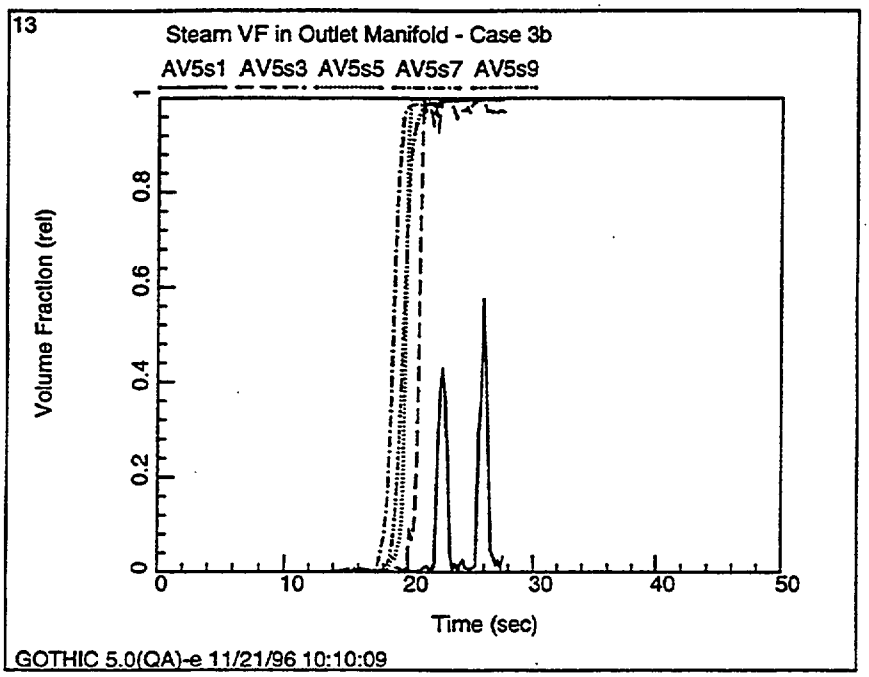

Figure A24. Steam Volume Fraction in Outlet Manifolds - Case 3b

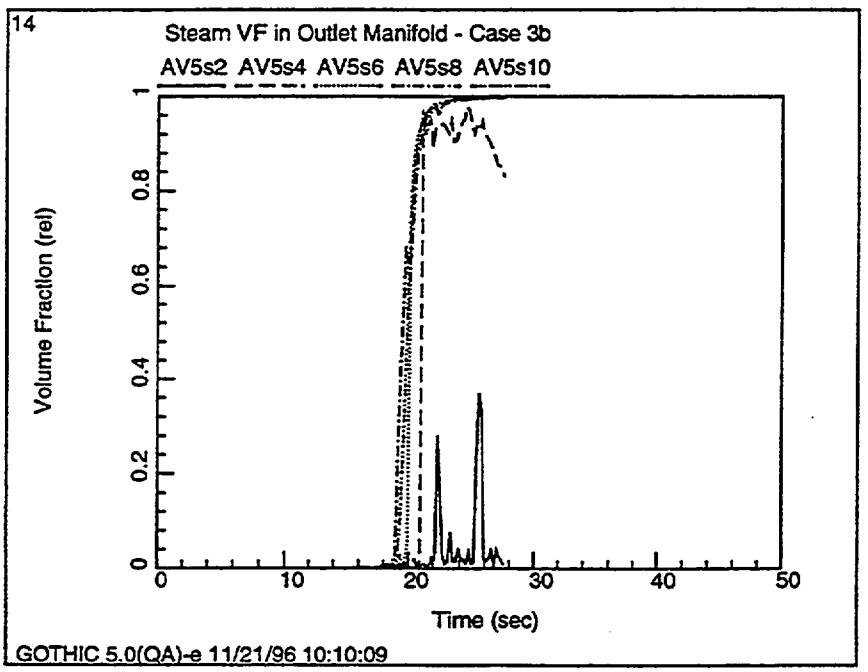

Figure A25. Steam Volume Fraction in Outlet Manifolds - Case 3b

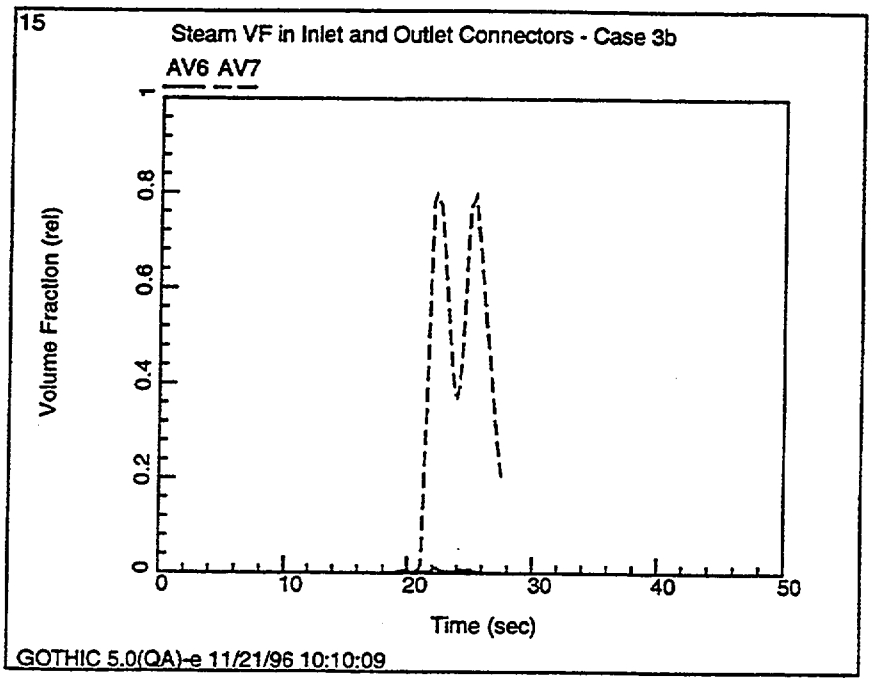

Figure A26. Steam Volume Fraction in Inlet and Outlet Connectors - Case 3b